UNIVERSITAT POLITÈCNICA DE VALÈNCIA

Escola Tècnica Superior d'Enginyeria Agronòmica i del Medi Natural

UNIVERSITAT POLITÈCNICA DE VALÈNCIA

School of Agricultural Engineering and Environment

Role of PLCB3 in adipogenesis

End of Degree Project

Bachelor's Degree in Biotechnology

AUTHOR: Montes Velástegui, Francisco

Tutor: Porcel Roldán, Rosa Caridad

External cotutor: Carobbio, Stefania

Experimental director: Navarro Pérez, Jaime

ACADEMIC YEAR: 2023/2024

TITLE

Role of PLCB3 in adipogenesis

ABSTRACT

Obesity is a medical condition associated with a higher risk of metabolic and cardiovascular complications, known as comorbidities. Around 15-45% of obese individuals are not affected by this kind of complications, the so-called “metabolically healthy obese” (MHO). In contrast, around 6-30% of the lean individuals present comorbidities comparable to the ones from obese patients, known as “metabolically obese normal weight” (MONW). In order to elucidate the biology underlying these paradoxical phenotypes, our research group has previously performed a collaborative genome wide association study (GWAS) to identify novel genes that predispose to obesity, but paradoxically have protective effects on cardiometabolic health, identifying over 60 adiposity-increasing loci with protective cardiometabolic effects. One of the genes found was PLCB3 associated with one two trait-pair (BMI-TG and BMI-HDL). Phosphatidylinositol-4,5-bisphosphate phosphodiesterase beta-3 is an enzyme encoded by the PLCB3 gene. It catalyses the formation of inositol 1,4,5-trisphosphate and diacylglycerol from phosphatidylinositol 4,5-bisphosphate. Genetic variants in PLCB3 gene have recently been identified as possibly regulating lipid homeostasis and body fat distribution in relation to adipose tissue expandability capability. Given all this evidence, in this work, we will investigate the role of PLCB3 depletion in the differentiation process from preadipocytes to mature adipocytes using the murine adipocyte 3T3L1 cell line. First of all, we made a bioinformatic analysis to obtain a preliminary Plcb3 expression profile. Next, we obtained the expression profile at mRNA and protein levels of this gene during differentiation in physiological conditions. Then, we will deplete Plcb3 in 3T3L1 cell line using a lentiviral shRNA approach. The cells will be then differentiated into mature adipocytes. At different stages of differentiation, molecular analysis will be carried out by qPCR and by immunoblot and morphological analysis by immunofluorescence. The obtained results suggest how Plcb3 could potentially play a role in adipogenesis, as it is seen both in bioinformatic analysis and mRNA/protein expression profiles how the gene expresses during adipogenesis in the early stages. Further, more specific results point towards Plcb3 having a possible dual role in adipogenesis regulating the expression of early adipogenesis genes (Pparγ2 and Cebpα) whilst it apparently promotes the expression of late expression lipid droplet formation genes such as (Ap2, Plin1 and Plin2). *Ki67* mRNA analysis results appeared contradictory with the protein analysis; therefore, morphological results appeared to be very helpful in validating mRNA Ki67 proliferation marker expression results. This points towards Plcb3 also having a role in the regulation of adipocyte proliferation. It is concluded that Plcb3 gene could have dual role in downregulating early adipogenesis genes whilst upregulating late adipogenesis genes.

KEYWORDS

3T3-L1, Adipocyte differentiation, comorbidities, obesity, Plcb3 and white adipose tissue.

TÍTULO

El papel de PLCB3 en la adipogénesis

RESUMEN

La obesidad es una condición médica asociada con un mayor riesgo de complicaciones metabólicas y cardiovasculares, conocidas como comorbilidades. Alrededor del 15-45% de los individuos obesos no se ven afectados por este tipo de complicaciones, la llamada "obesidad metabólicamente saludable" (MHO). En contraste, alrededor del 6-30% de los individuos magros presentan comorbilidades comparables a las de los pacientes obesos, conocidas como "peso normal obeso metabólico" (MONW). Con el fin de elucidar la biología subyacente a estos fenotipos paradójicos, nuestro grupo de investigación ha realizado previamente un estudio colaborativo de asociación genómica (GWAS) para identificar nuevos genes que predisponen a la obesidad, pero paradójicamente tienen efectos protectores sobre la salud cardio metabólica, identificando más de 60 loci adiposidad-aumento con efectos cardio metabólicos protectores. Uno de los genes encontrados fue PLCB3 asociado con un par de dos rasgos (BMI-TG y BMI-HDL). El fosfatidilinositol-4,5-bisfosfato fosfodiesterasa beta-3 es una enzima codificada por el gen PLCB3. Cataliza la formación de inositol 1,4,5-trisfosfato y diacilglicerol a partir de fosfatidilinositol 4,5-bisfosfato. Las variantes genéticas en el gen PLCB3 se han identificado recientemente como la posible regulación de la homeostasis lipídica y la distribución de la grasa corporal en relación con la capacidad de expansión del tejido adiposo. Dada toda esta evidencia, en este trabajo, investigaremos el papel de PLCB3 en el proceso de diferenciación de preadipocitos a adipocitos maduros de la línea celular murina de adipocitos 3T3L1. En primer lugar, realizaremos un análisis bioinformático para obtener un perfil de expresión Plcb3 preliminar. A continuación, obtendremos el perfil de expresión a nivel de ARNm y proteína de este gen durante la diferenciación en condiciones fisiológicas. Entonces, agotaremos PLCB3 en líneas celulares 3T3L1 usando un acercamiento lentiviral del siRNA. Las células entonces serán diferenciadas en adipocytes maduros. En diferentes etapas de diferenciación, el análisis molecular será realizado por qPCR y por inmunoblot y análisis morfológico por inmunofluorescencia. Los resultados sugieren cómo Plcb3 potencialmente podría tener un papel en la adipogénesis, ya que se ve tanto en el análisis bioinformático y los perfiles de expresión de ARNm/ proteína cómo se expresa el gen durante la adipogénesis en las primeras etapas. Además, los resultados más específicos apuntan hacia Plcb3 que tiene un posible papel dual en la adipogénesis que regula la expresión de los genes de la adipogénesis temprana (Pparγ2 y Cebpα), mientras que aparentemente promueve la expresión de genes de formación de gotas de lípidos de expresión tardía, tales como (Ap2, Plin1 y Plin2). Los resultados del análisis de ARNm y proteína para el gen Ki67 son contrarios, por lo que los resultados del análisis morfológico parecen ser muy útiles para validar resultados de expresión de marcadores de proliferación de ARNm en Ki67. Esto apunta a que Plcb3 también tiene un papel en la regulación de la proliferación de adipocitos. Se concluye que Plcb3 puede tener un papel dual en la represión de genes tempranos mientras promueve la expresión de genes tardíos de la adipogénesis.

PALABRAS CLAVE

3T3-L1, diferenciación de adipocitos, comorbilidades, obesidad, PLCB3 y tejido adiposo blanco.

ACKNOWLEDGEMENTS

Since I started my TFG journey on October 2024, I have felt incredibly proud of having the opportunity of being part of the I-76 team and learning from them. For this I feel very thankful towards Dr Stefania Carobbio which not only accepted and welcomed me to her team, but also guided me in the most wise and intelligent ways possible. I am also very thankful towards Dr Rosa Caridad Porcel Roldán from UPV, for being kind and welcoming when accepting me as her TFG student and also for her wise recommendations. I would also want to thank Jaime Navarro Perez for showing me all the knowledge I required to complete the project, for guiding me proactively throughout the journey of the TFG and also for being kind and patient with me, I wish you the best with your last year of PhD. I cannot forget the contributions of the rest of the team members: Dr Carmen Navarro Gonzalez, Alicia Enriquez de Salamanca Soto and the recent incorporation Dr Maria Martí Grau. Carmen and Alicia have been very kind, helpful and patient with me and have shown interest in the project. Even though Dr María Martí is relatively new in the team, she has also shown interest in my project and has proactively suggested ways in which I could improve my defence. Finally, I would like to thank one of our lab collaboratives Dr Antonio Puig Vidal which has also contributed with his knowledge on the project. The presence and contribution of all of these professionals has most certainly showed me many things I didn't know about handling myself in a lab environment and the process of developing and defending scientific projects.

However, there is a separate group of individuals for which I feel gratitude for their help and support during the projects journey. Here I would like to mention my mom and dad, my older and younger brothers, Rafa and Miguel for believing in me and cheering me up whenever I was feeling tired or depressed during this last year of my degree. I would also want to thank some of my close friends of school (Martín, Juan, Roberto, Manuel, Juanjo and Cristina) as wells as my UPV university friends from Karricocheo, Sapotaco group and my UCV friends from biotechnology (Adriá, Ángela, María and Óscar). I feel proud of being your friend and lucky for having you all in my life, as I am sure these years would have been worse without all of you. I would finally want to thank my personal trainer and friend Victor as well as Manuel which have shown great interest in my gym journey and have supported me inside an outside of the gym.

CONTENIDO

1 INTRODUCTION

1.1 ADIPOSE TISSUE AND ADIPOCYTES

Adipose tissue (AT) is a form of loose connective tissue which includes adipocytes and pre-adipocytes surrounded by an extracellular matrix as well as macrophages and endothelial cells. Both of these adipocyte statuses have different functions. Pre-adipocytes originate from the commitment of multipotent mesenchymal cell precursors called “Adipose-derived stem cells” (ADSC´s) (1). Pre-adipocytes are immature adipocytes and can differentiate onto mature adipocytes. They are numerically inferior to mature fat cells and from them new mature adipocytes can be generated when needed. Preadipocyte differentiation into mature adipocyte can be induced through several signalling routes such as hormonal signalling including growth factors, insulin, insulin-like growth factor and several steroid hormones as well as cytokines (2). Mature adipocytes are the main cell type in adipose tissue which play an important role in maintaining its homeostasis by regulating the balance between lipid storage as Triacylglycerol’s (TAGs) and lipids breakdown for energy consumption (3). TAGs can be used to obtain energy through their breakdown into fatty acids first and then their oxidation in the mitochondria (4). Besides its nutrient’s storage function, the AT plays many other crucial roles such as regulating insulin sensitivity and is an important secretory tissue. It releases adipokines or exosomes that contribute to the crosstalk between the different cell types that constitute it and its interaction with other organs through paracrine and endocrine effects (Figure 1).

WAT has been strongly linked with obesity and the development of its related comorbidities (3). For this reason, the following study will be focused only on white adipose tissue cells.

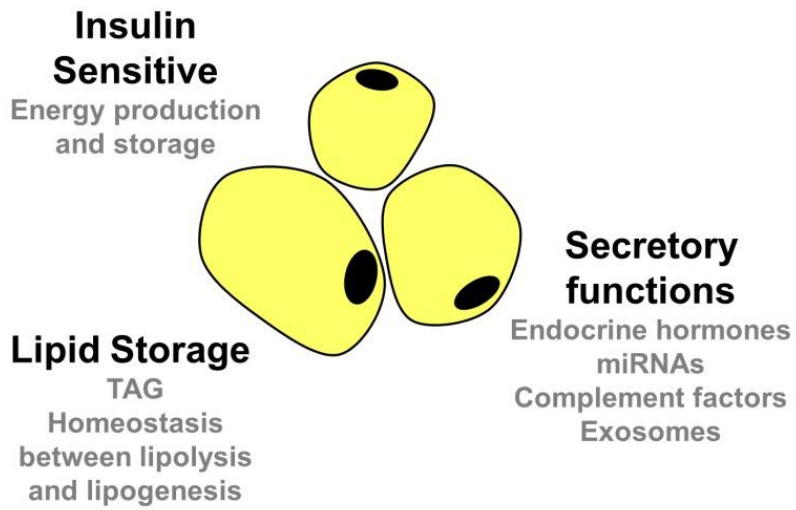

FIGURE 1: ADIPOCYTE FUNCTIONS. - ILLUSTRATION OF WHITE ADIPOSE TISSUE (WAT) CELLS ACCOMPANIED BY A LIST OF WAT MAIN FUNCTIONS – IMAGE EXTRACTED FROM: ALLISON J. RICHARD ET AL. 2020

Adipocytes can be distinguished in four separate classes: white, brown and two more, recently discovered classes, beige and pink (Figure 2); these adipocytes compose different types of adipose tissues. The White Adipose tissue (WAT) is the most abundant in the organism and is composed of classic adipocytes with a primary focus on energy storage. They are large and spherical (up to

100µm diameter), containing large unilocular droplets full of lipids inside. In addition to this, there are mainly two subtypes of WAT, subcutaneous WAT and visceral WAT (2). In humans, subcutaneous WAT is primarily present in abdominal and gluteal-femoral regions whilst visceral WAT is located primarily in the intra-abdominal area, surrounding inner organs. The Brown Adipose Tissue (BAT) is composed of adipocytes specialised in producing heat to maintain core body temperature. They have a reduced diameter (10-50um) compared to the WAT ones and use energy from their small multilocular lipid droplets to generate heat in their numerous mitochondrias (2). Mitochondrial heat production is specifically regulated by a key factor called UCP1, a mitochondrial inner membrane protein which is specific of brown adipocytes. UCP1 forms a pore in the inner mitochondrial membrane, which dissipate the proton gradient. As a result of this, ATP synthesis is blocked, and excess mitochondrial energy is released as heat (5). Additionally, to WAT and BAT, we have beige Adipose Tissue (bAT) and Pink Adipose Tissue (PAT). bAT adipocytes display features of both white and brown adipocytes. They are able to produce heat from the mitochondria when under proper stimulation and at unstimulated state, they resemble white adipocyte with a unilocular lipid droplet. Interestingly, there is existing evidence pointing towards the theory that WAT adipocytes can transdifferentiate into beige cells (6,7). Pink adipocytes are a novel kind which are located near the mammary glands. They are characterized by the presence of both milk droplets and lipid droplets, as well as cytoplasmic projections which give them epithelial like features (Figure. 2). They are characterized by the presence of both milk droplets and lipid droplets, as well as cytoplasmic projections which give them epithelial like features (Figure. 2).

FIGURE 2: THE 4 DIFFERENT ADIPOCYTE TYPES- ILLUSTRATION OF THE FOUR DIFFERENT ADIPOCYTE TYPES AND THEIR MORPHOLOGICAL AND INTRACELLULARFEATURES, WAT CELLS (TOP LEFT) ARE CHARACTERISTIC BY THEIR BIG SIZED LIPID DROPLET. BAT TISSUE (TOP RIGHT) IS CHARACTERISTIC BY ITS MANY SMALL LIPID DROPLETS AND ITS LARGE NUMBER OF MITOCHONDRIA'S. BEIGE FAT (BOTTOM LEFT) IS SIMILAR TO BAT BUT DIFFERS IN ISOME OF ITS LIPID DROPLETS SIZE, HAVING SOME THAT ARE OF GREATER SIZE THAN IN BROWN ADIPOCYTES. PINK ADIPOCYTES (BOTTOM RIGHT) ARE CHARACTERISTIC FOR THEIR EPITHELIAL-LIKE MORPHOLOGY AND MILK DROPLET PRESENCE. – IMAGE EXTRACTED FROM: ALLISON J. RICHARD ET AL. 2020

1.2 FROM STEM CELLS TO MATURE ADIPOCYTES

As commented in section 1.1, pre-adipocytes originate from the commitment of multipotent mesenchymal cell precursors (ADSC´s) (1). Pre-adipocytes are immature adipocytes and can differentiate onto mature adipocytes. Mature white adipocytes are formed through the process known as adipogenesis. The process of adipogenesis is controlled by the master regulator gene *Pparγ*. *Pparγ* expression is therefore vital for adipocyte differentiation. *Pparγ* acts by promoting the expression of adipogenic genes (*Ap2*/*Fabp4, Fasn, GLUT4* or *Plin1*) which promote growth and differentiation of adipocytes (8). Throughout the differentiation of preadipocytes into mature

adipocytes, there is a number of genes which are expressed at different stages of the process, and that can be used as markers of differentiation such as: *Pparγ2*, *Plin1*, *Plin2*, *Ap2* or *Cebpα*. The cell line used in this project, the 3T3-L1 murine cell line, is a preadipocyte cell line. Although committed, adipose tissue stem cellsstill maintain fibroblast morphology and therefore are easily distinguished from differentiated adipocytes by microscopy. Preadipocyte state is marked by *αSMA*, *PDGFRα/PDGFRβ*. Committed pre-adipocytes can be distinguished from non-committed ones by *ZFP423* marker. Once committed, pre-adipocytes can start to differentiate, adipocyte differentiation start is marked by both growth arrest and *PPARγ* master regulator gene expression activation (fig.3). During differentiation there are early differentiation expression markers such as *PPARγ*, *C/EBPα*, *C/EBPβ*, *AP2* and *GLUT4* (9) (fig.3). *AP2* (also known as *FABP4*) is a gene that codes for Adipocyte binding protein 2, which is a cytosolic protein which binds to long chained fatty acids and other lipid ligands. *AP2* protein has a role in lipid transport and metabolism (9). Even though *Ap2* can be described as an early adipogenesis gene for its early expression, its participation and peak expression starts on the later days of adipogenesis. *GLUT4* gene is highly expressed in adipose tissue and codes for an insulin-sensitive glucose transporter transmembrane protein (10). In differentiated adipocytes, we can observe the expression of different maturation markers such as: *PLIN1*/*PLIN2* (perilipins), *ATGL*, *LPL*, adiponectin or leptin (fig.3). *PLIN1* codes for perilipin 1 protein, which acts in mature adipocytes by coating and protecting lipid droplets (11). Perilipin 2 also acts protecting lipid droplets, although whereas *PLIN1* is expressed on the periphery of most lipid

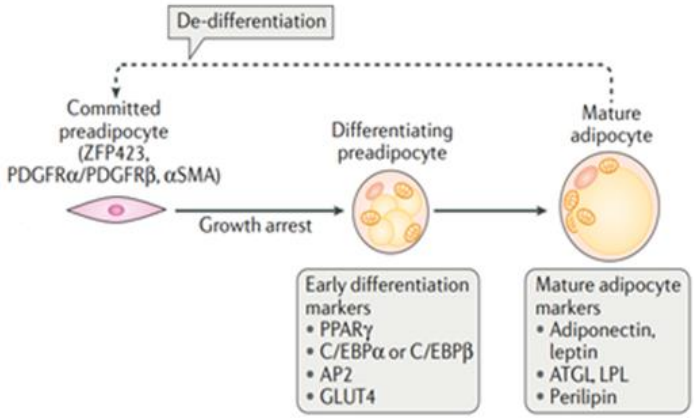

droplets, *PLIN2* is mostly expressed in small size lipid droplets which are located next to the cell nucleus or at cell periphery (12).

FIGURE 3: ADIPOGENESIS PROCESS IN 3T3-L1 CELLS. PREADIPOCYTE STAGE CAN BE DIFFERENCED FROM MATURE DIFFERENTIATED ADIPOCYTES BY ITS FIBROBLAST CELLULAR MORPHOLOGY AND EARLY PREADIPOCYTE DIFFERENTIATION MARKERS SUCH AS PPARΓ, C/EBP, AP2 OR GLUT4. MATURE ADIPOCYTES ARE DISTINGUISHED BY THEIR EXPRESSION OF MARKER GENES SUCH AS PLIN1 OR PLIN2 (PERILIPIN), ATGL, LPL, ADIPONECTIN LEPTIN – IMAGE EXTRACTED FROM: ADIPOGENESIS AND METABOLIC HEALTH BY ALEXANDRA L. ET AL

1.3 WHAT CAUSES OBESITY?

Obesity is a complex multifactorial condition influenced by both environment/lifestyle and genetic factors. This condition is known for its relationship with other comorbidities, such as: Type 2 diabetes mellitus and cardiovascular diseases (CVD) which include: atherosclerosis, hypertension or stroke (13). Obesity is not only influenced by lifestyle. In this case, genetic factors can affect the condition and could be playing a key role in its development. For instance, genetic variables could be behind the different obesity phenotypes and if so, they can greatly affect the impact of obesity on health of different individuals as for the chances of suffering from obesity comorbidities. For instance, it is known of the existence of epigenetic factors affecting development of obesity, such

as methylation of key metabolic genes or histone modifications. Obesity by itself can be harmful because the additional body weight creates big joint tensions which can cause lesions and even lead to osteoarthritis if joint tissue is heavily damaged. In addition to joint damage, obesity is known to cause chronic, low grade-inflammation (14), which can also lead to tissue damage or weakening in joints (15). Obesity is caused in first instance by an accumulation of body visceral or subcutaneous fat, being visceral fat more related to associated comorbidities (14). Genetic and epigenetic factors of obesity must not be downplayed, as they have the potential to be early disease markers and give us more insights over the disease's mechanisms (16). The combined use of GWAS (Genome wide association study) studies and projects such as this TFG will give more future insights on possible relations between genetic variables and obesity.

Obesity acts as an increasingly popular health threat in our society. We can see this trend reflected over obesity incidence in countries such as United States of America (USA) or Spain. In Spain, 2020 data statistics from INE (Spanish national statistics institute) extracted from population of 18 or more years showed approximately 44.9% of men were overweight, being 16.5% obese whilst in women 30.6% were overweight from which 15.5% were obese (17). In the other hand, in USA, 2021 statistical data from CDC-NHANEs showed approximately for adults of both sexes ranging from 40-56 years old 44,3% were obese and for ages ranging from 20-39 of both sexes 39.8% were obese (18). The frightening truth about this data is not only the fact that a big sector of our society is suffering obesity, but the fact that its prevalence is increasing alarmingly over time.

1.4 DIAGNOSTIC METHODS

Currently, the most widely used method of diagnosing obesity is the use of body mass index (BMI) (19). BMI is calculated by dividing the body weight in kilograms over the square of height in metres of a patient (20). BMI boundaries have been set to classify individuals into four main categories: Underweight (BMI < 18.5), normal weight (BMI: 18.5-24.9), Overweight (BMI: 25-29.9) and Obese (BMI > 30). Using BMI as a diagnostic tool has some advantages as its use is very popular, it's simple to calculate and, although it is does not measure direct amount of body fat, its measurements are usually associated with it. BMI might be a useful tool for classifying individuals' degree of obesity, but it does not measure body fat mass directly and it also doesn't separate visceral from subcutaneous fat. These limitations indicate that BMI is not enough by itself to measure degree of obesity accurately. An example of these limitations are bodybuilders, which have an obese-like BMI although they don't have excess fat, meaning the technique can't differentiate muscle mass from fat mass excess. It is also very important to highlight that fat measurements can discriminate visceral fat from subcutaneous fat, as it is known that visceral fat is more damaging to health and associated to diseases than subcutaneous fat (14). To tackle these limitations, BMI measurements could be accompanied by further Bioimpedance and/or height to waist ratio measurements (21). For distinguishing visceral from subcutaneous fat, CT scans and magnetic resonance provide accurate measurements (21).

1.5 DIFFERENT FORMS OF OBESITY

Obesity is a heterogeneous multifactorial condition in which individuals with similar BMI´s have different metabolic and CVD risk profiles. The heterogeneity comes from differences across individuals of different sex, age, race, diet/lifestyle and genetic background. These differences can be measured by use of omics techniques such as: transcriptomics, microbiome analysis,

metabolomics, proteomics and genomics (22). One of the strongest proofs of the importance of genetic variables in obesity is the existence of different phenotypes related to it, as there are individuals which are healthy and obese, other that are unhealthy and obese, as well as others suffering obesity-associated comorbidities whilst not being obese. There have been described four different phenotypes related to obesity: Metabolically healthy normal weight (MHNW), Metabolically normal weight (MUNW), Metabolically healthy obese (MHO) and metabolically unhealthy obese (MUO) (Figure 4). Obese individuals can be separated from non-obese by earlier mentioned diagnostic techniques such as BMI. Healthy individuals can be separated from unhealthy presence/absence of obesity comorbidities and by measurement of visceral fat, measurement of LDL/VLDL cholesterol levels as well as HDL levels, insulin resistance, disglycemia (abnormal blood sugar levels) and blood pressure which allows to create the healthy/unhealthy profile (16). MHO have been described as having lower risk of developing type 2 diabetes mellitus or CVD as they remain insulin sensitive and less adipose tissue inflammation is observed. Evidence from animal models shows that MHO group is healthier because they tend to accumulate less visceral fat and more subcutaneous fat (16). MUNW is another interesting group, as despite having normal BMI they suffer from comorbidities. It has been seen that specially over Asian or Asian American populations have a greater tendency of accumulating visceral fat, resulting on individuals with normal BMI suffering from obesity-related conditions (16). MUNW phenotypes also raise questions about BMI efficacy in obesity diagnosis and suggests that a different BMI range should be included for diagnosis of different ethnic groups to differentiate obese from normal weight. In addition to this, separation of phenotypes for healthy and non-healthy is actually non-standardised, but MUO could be separated from MHO (or MUNW from MHNW) by earlier commented metrics such as HDL levels, insulin resistance and blood pressure. In this sense, a previous GWAS (23) comparing the different obesity phenotype populations have resulted in the discovery of 62 loci with alleles statistically associated with higher adiposity and lower cardiometabolic risk, which would be related with a metabolically healthy obese phenotype (MHO). From this previous study (23), *PLCB3* is one of the discovered genes associated to an MHO phenotype because of its statistical relation to high HDL levels and low triglyceride levels as well as promoting fat development (23). Therefore, in this study we aim to investigate the role of *PLCB3* in adipogenesis.

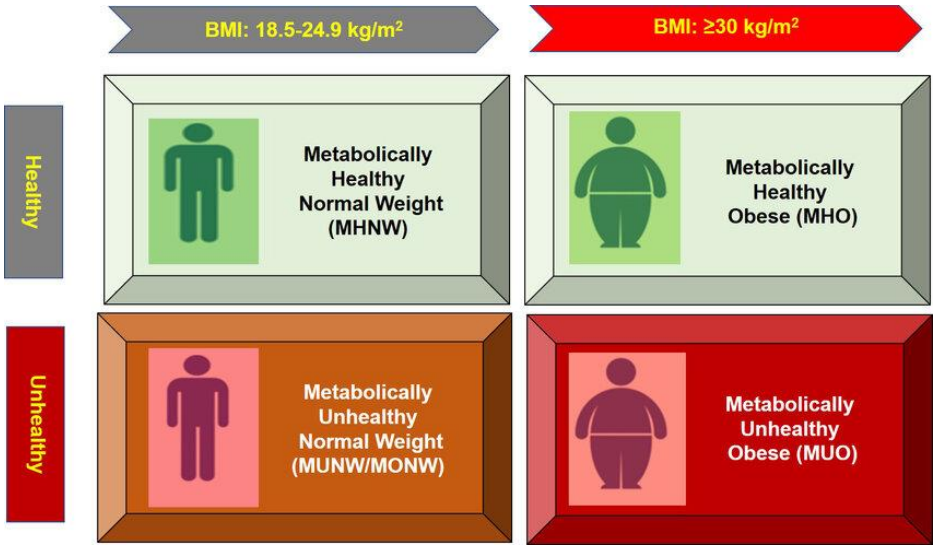

FIGURE 4: THE FOUR DIFFERENT OBESITY PHENOTYPES- ILLUSTRATION SHOWS THE DIFFERENT OBESITY PHENOTYPES, WHICH ARE SEPARATED INTO FOUR CATEGORIES BY HEALTHY/UNHEALTHY AND BY BMI DATA. OF NORMAL WEIGHT ARE CONSIDERED THOSE

PEOPLE WHO ARE NOT OVERWEIGHT OR OBESE (BMI:18,5-24,5). CRITERIA FOR SEPARATING HEALTHY AND NON-HEALTHY INDIVIDUALS ARE NOT SPECIFIED, AS IT THEY ARE NON-STANDARDISED, ALTHOUGH THERE ARE SOME CRITERIA WHICH ARE RECOMMENDED FOR THAT SUCH AS MEASURING VISCERAL FAT, CHOLESTEROL LEVELS AND INSULIN RESISTANCE. THEREFORE, WITH THESE CRITERIA, METABOLICALLY HEALTHY INDIVIDUALS (TOP LEFT) ARE THOSE WHO HAVE A NORMAL BMI AND HEALTHY CONDITIONS, METABOLICALLY UNHEALTHY NORMAL WEIGHT (BOTTOM LEFT) ARE INDIVIDUALS WHICH SUFFER FROM OBESITIES ASSOCIATED COMORBIDITIES WITHOUT BEING OBESE. METABOLICALLY HEALTHY OBESE (TOP RIGHT) INDIVIDUALS ARE THOSE THAT ARE OBESE BY BMI BUT DON'T SUFFER FROM OBESITIES COMORBIDITIES. METABOLICALLY UNHEALTHY OBESE INDIVIDUALS (BOTTOM RIGHT) ARE THOSE WHICH ARE BOTH UNHEALTHY AND OBESE BY BMI. – IMAGE EXTRACTED FROM: KAISER A. WANI ET AL

1.6 PLCB3 GENE

PLCB3 gene belongs to a family of 13 membrane bound phospholipase proteins. All protein family members can be grouped in six classes: β, γ, δ, ε, η and ζ. All PLC family members share the same core domains except PLC ζ, which lacks the PH (Pleckstrin homology) domain. The *PLCB3* gene encodes for phospholipase C beta subunit variant 3 (PLCB3) protein and in humans its located on the 11th chromosome at position 11q13.1 (24). PLCB3 activity is dependent of g-protein activation by alfa g-protein. At the same time g-protein activation is coupled to g-protein coupled receptors (GCPRs). It is important to note that GCPRs are not the only receptors which can activate PLCB3. Also, receptor such as T-cell receptors, B-cell receptors or integrin adhesion proteins can have the same effect. PLCB3 function is to catalyse the transformation of Phosphatidyl inositol 4,5 biphosphate (PIP2) into the second messenger's inositol 1,4,5 triphosphate (IP3) and Diacylglycerol (DAG). IP3 acts by opening calcium channels on endoplasmic reticulum (ER), which results in an increase in intracellular calcium. At the same time, Ca2+ activation through PLCB3 is known to regulate gene expression and promote proliferation, differentiation and growth amongst others. In the other hand, DAG acts by activating Ca2+ dependent protein kinase C (PKC) which is known for phosphorylating and activating downstream signalling effectors such as AKT, resulting in proliferation and cell differentiation amongst others (25) (Figure 5).

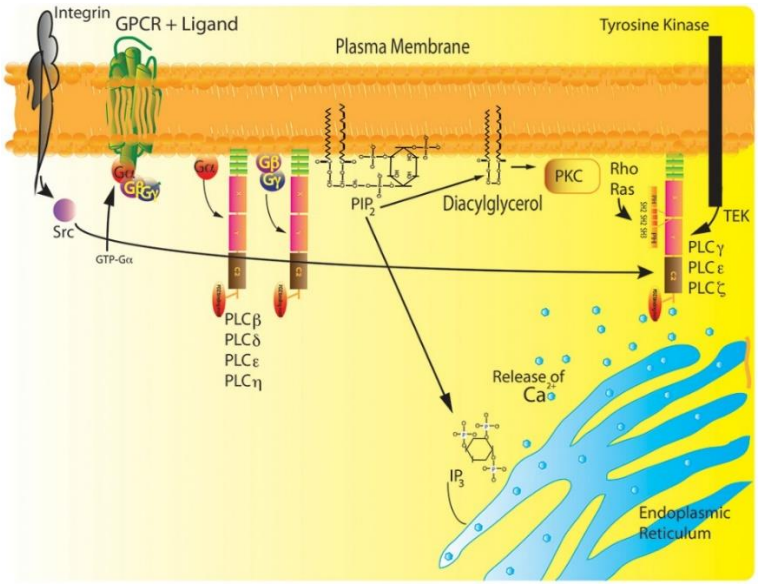

FIGURE 5: PLCB3 INTRACELLULAR ACTION MECHANISM – PLCB3 IS A MEMBRANE BOUND PROTEIN WHICH IS ACTIVATED VIA G PROTEIN ALFA SUBUNIT. IT CAN ALSO BE ACTIVATED BY OTHER MECHANISMS SUCH AS INTEGRIN SIGNALLING. ONCE ACTIVATED, PLCB3 CATALYSES THE BREAKDOWN OF ITS SUBSTRATE, PIP2 (PHOSPHATIDYL INOSITOL 4,5 BIPHOSPHATE) INTO THE SECOND MESSENGERS IP3 (INOSITOL 1,4,5 TRIPHOSPHATE) AND DAG (DIACYLGLYCEROL). IP3 ACTS INDUCING CALCIUM LIBERATION FROM ENDOPLASMIC RETICULUM STORES INTO CYTOPLASM. DAG ACTS ACTIVATING PKC (PROTEIN KINASE C) WHICH ACTS PHOSPHORYLATING AND ACTIVATING GENE EXPRESSION REGULATORS OF CELL FUNCTION. – IMAGE EXTRACTED FROM COLIN A. BILL ET AL.

PLCB can is subjected to alternative splicing resulting in 4 different splicing variants: PLCB1 (150kDa), PLCB2 (140kDa), PLCB3 (152kDa) and PLCB4 (130kDa) (25). In addition to this, all splice variants, except PLCB3, have further splice variants, creating sub-isoforms such as PLCB1a and PLCB1b. All PLCB splice variants possess the same catalytic core but differ primarily in their X-Y linker domain length, but also in with respect to the CTD linker length and extreme C terminus length (26). PLCB3 catalytic core protein domains include PH, EF hands, X-Y linker, C2 and the TIM barrel. The TIM barrel domain acts as the active site and it's split in the gene sequence into X and Y domains, having the X-Y linker in between (Table1; Figure 6).

TABLE 1: PLCB3 PROTEIN DOMAINS FUNCTIONS

PLCB3 protein domain	Domain function
PH domain	Binds to PIP2 substrate with high affinity at active site
EF hands	Calcium independent and serve as scaffold
X-Y linker	Blocks active site (autoinhibition)
C2	Intra and intermolecular regulatory binding sites
TIM barrel (divided in X and Y)	Active site
Distal CTD	Binds N-terminal of G alfa protein and to the cell membrane
Proximal CTD	Primary G alfa protein binding site
CTD linker	Links and separates proximal and distal CTD

Under normal circumstances the active site at TIM barrel domain is blocked by the X-Y linker, maintaining the enzyme inactive. When a g-protein coupled receptor (GPCR), on the cell membrane, is stimulated, the g-protein alfa subunit is activated and migrates across the membrane to activate PLCB3. Alfa g-protein interacts with distal and proximal CTD domains, inducing a conformational change which displaces X-Y linker from the actives site and activates the enzyme. Now PIP2 substrate is free to bind to PH domain at the active site (fig 6.B) and is transformed into IP3 and DAG secondary messenger products (26).

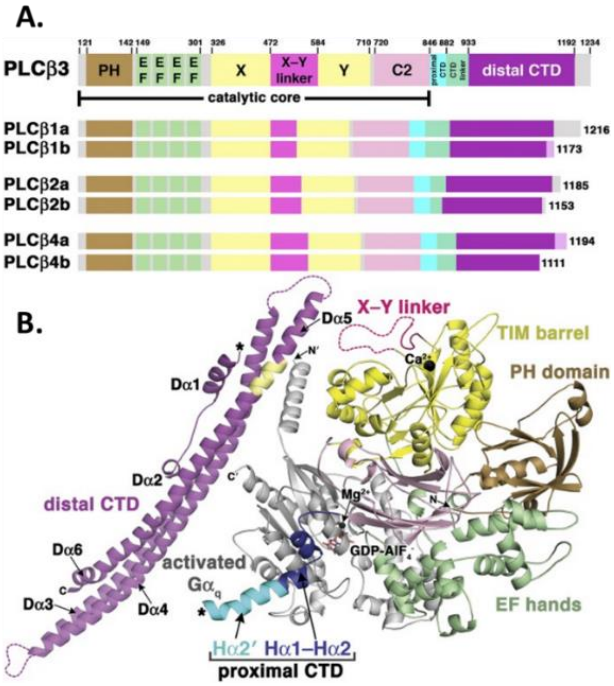

FIGURE 6: STRUCTURE AND SEQUENCE ORGANISATION OF PLCB3 GENE AND PROTEIN. A: PLCB3 GENE SPLICING VARIANTS- THE ILLUSTRATION SHOWS PLCB GENE SPLICE VARIANTS, RESULTING IN PLCB1,2,3 AND 4 WHICH ARE MAINLY DIFFERENTIATED BY LENGTH IN X-Y LINKER DOMAIN, DISTAL CTD DOMAIN AND EXTREME C TERMINUS DOMAIN LENGTH. EACH SPLICE VARIANT CAN HAVE ITS OWN SUB-SPLICE VARIANTS, EXCEPT PLCB3, GIVING AS RESULT FORMS A AND B. IN ADDITION TO THIS, CATALYTIC CORE DOMAINS ARE HIGHLIGHTED, INCLUDING: PH DOMAIN (BROWN), EF HANDS (GREEN), TIM BARREL (SEPARATED IN X AND Y YELLOW DOMAINS), X-Y LINKER (PINK) AND C2 DOMAIN (LIGHT PINK). B: PLCB3 PROTEIN STRUCTURE DOMAINS- THE ILLUSTRATION SHOWS THE 3D STRUCTURE OF PLCB3 PROTEIN WHERE SPATIAL LOCATION OF DOMAINS CAN BE SEEN. DOMAINS HAVE THE SAME COLOUR CODE USED IN FIGURE 6.A. IN THIS FORM THE PROTEIN IS INACTIVATED AS X-Y LINKER (PINK) IS SEEN BLOCKING THE ACTIVE SITE OVER AT TIM BARREL DOMAIN (YELLOW). DISTAL CTD MEMBRANE BOUND DOMAIN (PURPLE) IS VISIBLY SEPARATED FROM THE REST OF THE PROTEIN. THE PROXIMAL CTD (LIGHT AND DARK BLUE) IS ALSO LOCATED FURTHER FROM THE ACTIVE SITE AND THE SITE WHERE ACTIVATED GA PROTEIN WOULD JOIN (MARKED WITH AN ASTERISK). PROXIMITY OF SUBSTRATE BINDING PH DOMAIN (BROWN) TO THE ACTIVE SITE CAN ALSO BE OBSERVED. – IMAGES MODIFIED FROM: STRUCTURAL INSIGHTS INTO PHOSPHOLIPASE C-B FUNCTION BY ANGELINE M. LYON ET AL.

1.7 *IN VITRO* AND *IN VIVO* MODELS FOR WAT STUDY

There are several in vitro models for WAT that allow us to get a better understanding of its physiology and to develop new therapeutic strategies. Within mouse WAT cell lines, there are 3 main types: 3T3, C3H and OP9. 3T3 cells are aneuploid fibroblast like cells that are sensitive to contact inhibition under confluence. C3H cells are similar to 3T3 cells as they are fibroblast-like aneuploid and sensitive to contact inhibition. Besides their similarities, C3H cells are mostly used for research in brown adipose tissue, as they have interesting browning characteristics (WAT cells transdifferentiating onto brown adipose tissue) that 3T3 cells don't have. From all variants of subclones of C3H cells, the subclone we could stand out C3H/10T1/2 has been specifically used for adipogenesis and brown adipocyte research. OP9 cell lines are characterised by their ability to differentiate in only 3 days. Other advantages of the OP9 cells include their capability to keep their adipogenic potential over time and passages, even if they are passed from confluent cells. OP9 cells are also easily transfectable using viruses as well as plasmids or siRNA, which makes a specially desired cell line for use of CRISPR-Cas9 gene editing (27). The cell line used in this TFG is a 3T3 cell line. There are 2 main 3T3 cell lines used for WAT: 3T3-L1 and 3T3-F442A cell lines. 3T3-F442A cells are similar to 3T3-L1, as they are both derived from murine swiss 3T3 cells. However, 3T3-F442A cells show a more advanced commitment within the adipose lineage. This is due to the fact that

they have been isolated from the selection of a third clone that presents higher size fat clusters and greater frequency of development of lipid droplets (28). However, 3T3-L1 cells are significantly more used than 3T3-F442A cells, it is suspected that this is due to the lower commercial availability of this cells (27).

3T3-L1 cells have some key advantages that have made them be the actual gold standard for adipocyte cell studies. The main advantages of these cells include easy maintenance, robust differentiation and high reproducibility. They are easy to maintain and grow in laboratories, this allows the possibility to make various experiments in parallel. In addition to this, they have a robust differentiation as they have the ability to be induced into adipocyte differentiation when exposed to specific chemical stimulation. This specific process gives the cells a high reproducibility, as they tend to have a very consistent behaviour when grown or differentiated (29).

Nevertheless, there are some disadvantages to the use of 3T3-L1 cells. The main disadvantages reside in the fact that these cells are a simplified model of adipose tissue that might not fully mimic the complexity of real adipose tissue and that there might be differences between human and mouse adipocytes as different species could not act in the same exact way (29)

It is also important to remember that, although not used in this project, there are in vivo models for obesity. Many in vivo obesity models are based on mice (*mus musculus*). Mice obesity models have shown to be reliable and effective, have a short generation interval and can generate large populations (30). Some of the most used in vivo obesity mouse knockout models are: ob/ob mice and db/db mice (31). Ob/ob mice are deficient in leptin food satiety hormone, resulting in mice that are hyperphagic and end up being obese even on chow diet administration, the effect is reversible if leptin is administered (31). Db/db mice are deficient in leptin receptor, which results in the same effect as ob/ob mice but in this case the phenotype is not reversible by leptin administration. However, there are also other interesting knockout mice models such as POKO mice which are mice lacking *Ppary* gene on an ob/ob background and therefore, present an impaired adipose tissue expandability. These modification results in POKO mice having high blood glucose and ectopic fat accumulation in other metabolically relevant organs (32).

2 HYPOTHESIS AND OBJECTIVES

2.1 HYPOTHESIS

Based on a collaborative GWAS study, *Plcb3* gene seems to be statistically correlated with MHO phenotype, meaning it can possibly promote adiposity but diminish the risk of developing metabolic complication. In addition to this, *Plcb3* gene contributes to activation of AMPK signalling pathway, which has been known to repress differentiation via Sox9 repressor and proliferation via p51/p21 and TSC. Therefore, our hypothesis is that *Plcb3* silencing could promote adipocyte differentiation, as well as regulate proliferation capability of the cells.

2.2 OBJECTIVES

The main objective of this study is to investigate the role of Plcb3 in adipocyte differentiation and proliferation.

1. Bioinformatic analysis to preliminarily profile *Plcb3* expression
2. *Plcb3* expression profile analysis in wild type conditions by mRNA expression analysis using RT-qPCR
3. Validation of *Plcb3* mRNA expression profile under wild type conditions using western blot analysis
4. To determine the effect of *Plcb3* gene silencing in the differentiation process by analysing the changes in mRNA and protein expression of key genes in adipogenesis (*Plin1*, *Ap2*, *Pparγ* ISO 1 and 2)
5. To determine the effect of *Plcb3* gene silencing in the proliferation of 3T3-L1 cells by analysing the changes in mRNA and protein expression of *Ki67*.
6. Validation of previous results with morphological analysis by immunofluorescence marking of *Plin1* at days 3 to 9 of differentiation and *Ki67* for day 1 of differentiation and staining of lipid droplets using LipidTOX at days 7 to 9.

3 MATERIALS AND METHODS

3.1 BIOINFORMATIC ANALYSIS

After a search in the public depository "gene expression omnibus" (GEO), the study GSE95533 is found. This study consists on an expression profiling by high throughput sequencing in 3T3-L1 cells during adipogenesis. Expression on the study was only measured for days 0, 4 hours, day 2 and day 7. One of the many genes included in the study is *Plcb3*. It was also interesting for this project as not only they use the same cell line but they also used the same differentiation cocktail. Once the raw data for *Plcb3* is extracted from GSE95533 the expression analysis is done using an R programme package called DESeq. From here, the programme uses a model based on negative binomial distribution to determine differential expression statistically within the imported data. P values obtained from the processing are adjusted using a Will-Coxon approach to control false discovery rate (FDR). Samples are adjusted for a P-value < 0,05 are assigned as differentially expressed. For the data Day 0 was compared to Day 7 and a P value of 0,33 is obtained. Obtained graphical results are represented in a boxplot using ggplot function.

3.2 CELULAR CULTURES

2D or 3D cell culture models are useful tools for scientific research purposes. In this project, the cell culture used is a 2D cell culture model formed of the 3T3-L1 cell line. 3T3-L1 cell line are adherent mouse fibroblast preadipocyte cells. This 2D model allows to study accurately the adipogenesis process from preadipocyes to mature adipocyte.

3.2.1 DEFROSTING OF THE CELLS

For cell defrosting, a vial of cells is taken from liquid nitrogen storage and put in a water bath at 37ºC to defrost for 2 minutes maximum, not dipping the O-ring and the cap of the vials in the waterbath to avoid possible contaminations. Once defrosted, the cells are transferred into a 15ml flacon tube with 10ml of supplemented DMEM high glucose medium (supplemented medium contents described under 3.2.2 maintenance section contents) and centrifuged for 2 minutes at

1200rpm. Once centrifuged, the supernatant with toxic DMSO is eliminated and the cell pellet is resuspended in 1ml of medium, then the cells are transferred into a T-75 flask with 15ml medium.

3.2.2 MAINTENANCE

Cells culture medium used is DMEM high in glucose (DMEM: Gibco, Waltham, MA, USA), supplemented with 10% Fetal Bovine serum (FBS), Glutamax (L-Glutamine: ThermoFisher Scientific, Walhtam, MA, USA) and Penicillin/Streptomycin (Pen/Strep) (ThermoFisher Scientific, Walhtam, MA, USA) antibiotics both at 1% concentration (DMEM supplemented). To ensure aseptic conditions throughout the experiment, cells are always handled under an II A class laminar flux hood (Telstar BIO II A class 2 biological safety cabinet: Telstar, Barcelona, Spain). The cell´s used are maintained in T-75 flasks which are located in an incubator (ThermoFisher Scientific, Walhtam, MA, USA) at 37ºC and 5% CO2. 3T3-L1 cells are adherent and susceptible of inhibition by contact. Therefore, the cells are passed into a different flask in a 1:10 dilution every 48h to 72h (70-80% of confluence). The cells are monitored using an inverted microscope *Leica DMi8* (ThermoFisher Scientific, Walhtam, MA, USA) daily to check confluence, any possible contaminations or cell culture abnormalities. The process of cell subculturing starts with the aspiration of culture media followed by a wash with 3ml of PBS, which will also be then aspirated. Furthermore, 2.5ml of trypsin of pre-warmed at 37ºC (ThermoFisher Scientific, Walhtam, MA, USA) are added to cells for 3 minutes in the incubator so that they detach from the flask. Next, trypsin is inactivated by addition of 2.5 ml of DMEM supplemented medium on to the cells. Then the flask content is pipetted up and down to ensure all cells have been detached from the surface. Following this, the cells need to be passed into a 15ml falcon tube and centrifuged for 2 minutes at 1200 rpm using an *Eppendorf 5415 R Centrifuge* (Eppendorf, Hamburg, Germany). Once the centrifugation is finished, the supernatant is aspirated and the pellet is resuspended in 5ml of medium. When the pellet is fully resuspended, 500µl of cells are transferred from the falcon tube into a new T-75 flask with 15ml medium, to obtain a 1:10 dilution. The flask is placed in the incubator in incubator (37ºC, 5% CO2). 3T3-L1 cell´s require media replacements every 48h.

3.2.3 FREEZING OF THE CELLS:

Firstly, for freezing the 3T3-L1 cells from a T-75 flask, the freezing medium needs to be prepared. The freezing medium includes FBS with 10% dimethyl sulfoxide (DMSO, ThermoFisher Scientific, Walhtam, MA, USA). Usually, from a T-75 flask 3-4 cryovials of cells can be frozen. Once the freezing media is prepared, the cells medium is aspirated and the cells washed with 3ml of PBS, which will be removed after wash. Then 2,5 ml of trypsin is added Then the trypsin is inactivated by addition of 2,5ml of supplemented DMEM and the flask content is pipetted up and down to ensure they are all detached. Next, the cells are passed into a 15ml falcon tube and centrifugated for 2 minutes at 1200rpm. The supernatant is then aspirated and the pellet is resuspended in 4ml of freezing media. After resuspension, 1ml of cells in freezing media is transferred into 4 cryotubes. Cryotubes are then transferred into a Mr Frosty (ThermoFisher Scientific, Walhtam, MA, USA) containing isopropanol and stored in a freezer at -80ºC for 24h. The use of Mr frosty ensures that cells temperature is slowly decreased to -80ºC in a pace of -1ºC/min. This procedure will ensure that the cell viability is preserved and not drastically affected by freezing. After 24h, cells are then transferred into liquid nitrogen tanks, allowing to preserve them at -196ºC for long periods of time.

3.3 LENTIVIRAL *PLCB3* GENE SILENCING

Gene silencing is a potent genetic expression modification tool that allows researchers to study the effect of the reduction of the expression of a certain gene in processes of interest.

For this project, *Plcb3* gene silencing was achieved by using stable lentiviral transfection. Viral particles include three important components in their genome: GFP gene, puromycin resistance gene and target sequence silencing transcript. Firstly, a MOI (multiplicity of infection) pilot experiment was performed with a range of viral concentrations to test the optimum viral concentration to use for the main experiment. The ideal MOI is selected so it contains is enough viral particles to infect 100% of cells, is small enough not to cause cell metabolism alterations or excessive cell stress and death. Viral samples are prepared in 1ml media as follow: infective silencing virus particles at set MOI concentration, DMEM supplemented with high glucose medium, glutamax and pen/strep antibiotics. The medium used do not contain serum as it can negatively affect the lentivirus infectivity capability, but contains polybrene 1ul/ml which promotes viral infectivity. Two 6 well plates with same sample order are set where 120,000 cells are grown per well. One plate is used for infection with the silencing virus and for infection with the non-target lentiviruses(control). Each 6-well plate has: 4 wells with different MOI viral concentrations (MOI1, 3, 5 and 10), a well for negative control with cells without virus and a well for counting cells. The cell counting well allows to calculate the MOI of each well (ratio of viruses to cells). The number of cells per well is calculated before transfection. The non-target lentivirus infects cells but the sequence for silencing that it carries do not codes for any existent transcript in the mouse genome and therefore will not silence any gene. The viral not targeting trascript plasmid, which will not interact with the mouse cell´s genome, will express GFP and puromycin resistance genes. That allow to monitor the effectivity of the infection of the cells. 24h after cells are seeded, the DMEM supplemented medium is washed and replaced by serum free DMEM high glucose medium. Next, cells are counted using the well in the plate allocated for cell counting. This allows to know the cells number and to determine the viral volume needed for each MOI. Next, the cells are infected with MOI concentrations of 1, 3, 5 and 10. The Cells are then incubated (37ºC, 5% CO2) for 4h, after which 100ul of serum will be added to each well and left overnight. Next day the cells are washed 3 times with DMEM supplemented medium and then 2ml of supplemented medium will be added to each well. The plate also includes a control well where there is no virus added, which allows to measure if the amount of polybrene used has being toxic to the cells or not. Finally, the infected cells are separated from the non-infected by either flow cytometry, sorting the GFP+ cells or puromycin selection. To separate the positively infected cells from the non-infected we used the flow citormetry approach, sorting the GFP+ cells. The cells infected with a MOI of 1 were discarded as no fluorescence was detected, leaving us with GFP+ cells infected with MOI´s 3, 5 and 10. After sorting, the GFP+ cells of the different MOIs are passed from their respective 6 well plate to a T-75 flask and are frozen following the protocol seen earlier (section 3.2.3). Once stable infected cells lines of each MOI are obtained, further analysis is required is required to decide which MOI concentration is ideal (lowest MOI with highest silencing) to perform the main experiment. For this, cells of each MOI are grown in a 12-well plate format. For each cell line will have 3 wells, two for RNA sample collection and one for protein collection. Once the cells have become confluent, RNA and protein samples are collected and analysed by q-PCR and western blot, respectively. The results of the qPCR and WB will show which virus MOI has produced lower *Plcb3* gene and protein expression for that reason, this is the ideal MOI to use for the main experiment.

3.4 3T3-L1 DIFFERENTIATION

The adipocyte differentiation process is key for the project as we want to elucidate how *Plcb3* gene affects its progression. 3T3-L1 preadipocyte differentiation takes 9 days. Taking this in count, to

study the process in depth, samples will be collected at days: 0, 1, 3, 5, 7 and 9. The experiments will be structured as follow: we will collect three biological replicates (N=4) per cell line (silenced and non-target), per day. For each replicate, cells are seeded into four 12 well plate from which 2 plates will be for non-target condition and the other two for the *Plcb3*-silenced condition. The two plates of each condition will be organised in the following structure: for each analysed day of the differentiation process there will be two wells for collecting RNA samples, one well for collecting protein samples, and a final well for immunofluorescence analysis, except for day 9 that will have two immunofluorescence wells instead of one.

To prepare cells for the differentiation process, approximately 70,000 cells are seeded per well containing 1ml of DMEM supplemented media. After this, cells are left to become confluent for 48h in an incubator (37ºC and 5% CO2). Once the cells become confluent, cell media is changed to DMEM supplemented again and the cells are left for other 2 days in the incubator (37ºC, 5% CO2). 48h after the confluency is reached, the differentiation process can start and we will refer to this day as day 0. To induce differentiation of the ells, 1ml of a differentiation cocktail including IBMX (0,5mM), dexamethasone (0,001mM) and insulin (0,005mM) is added to each well. After this, cells are left for 72h in the incubator (37ºC, 5% CO2). After these three days, day 3 samples are collected and the media is changed for media including: DMEM supplemented and insulin (0,005mM). After the media is changed, the cells are left for incubation (37ºC, 5% CO2) for another 72h. At day 6, the media is changed one more time, and it contains just DMEM supplemented. Finally, cells are left for incubation for 72h in the incubator and cell samples from day 7 and 9 will be collected on their respective days.

3.5 RNA HANDLING AND ANALYSIS

3.5.1 RNA SAMPLES COLLECTION

As mentioned earlier, on each of the days of differentiation indicated, for each day and experimental condition, an RNA sample was collected from 2 wells. To obtain the samples, process starts by aspirating cell media from the 2 wells and washing them with 320µl of PBS per well, which will then be aspirated after washing. Next, 160 µl of trypsin are added per well and cells are incubated for 3 minutes in the incubator (37ºC, 5% CO2). After incubation, trypsin is inactivated by adding 160 µl of supplemented media per well. Once trypsin is inactivated, it is made sure that all cells are detached from the plate by pipetting up and down. After this, the resuspended cells of both wells are transferred into a 1,5ml Eppendorf tube and are centrifuged at 1200 rpm for 2 minutes. Next, the supernatant is eliminated carefully by aspiration, making sure the pellet is not aspirated as well. Finally, the Eppendorf tubes with the RNA sample pellet is frozen by put it in dry ice and stored at -80ºC in the freezer.

3.5.2 RNA EXTRACTION:

The RNA extraction process starts by thawing the previously obtained cell pellets, by leaving them on ice. Next, 1ml of TRItidy G lysis reagent is added to each sample and the pellet is homogenized by pipetting the sample gently up and down. After this, the homogenized lysate is incubated for 5

minutes at room temperature. Once the incubation is over, 200 µl of chloroform are added, the sample is mixed by vortexing it and is incubated 10 minutes at room temperature. Next step is the centrifugation of the lysate at 4ºC for 15 minutes at 12000 rpms. When the centrifugation is over, 2 liquid phases separated by an interphase will be observed: an upper aqueous phase which includes the desired RNA, an interphase full of cellular debris and a lower phase of chloroform. In this step it is crucial to transfer the upper phase liquid into a new 1,5ml Eppendorf tube without touching the interphase´s contents, as they are contaminants that can disturb the later steps of the extraction. The following step involves RNA precipitation by addition of around 500µl of isopropanol to the RNA tube and leaving it in a -20ºC freezer overnight. The next day, the samples are centrifuged for 15 minutes at 4ºC and 12000g. Then, the RNA is washed twice with 1ml of ethanol 70%. After this first washing, the samples are vortexed until the RNA pellet is fully resuspended and after the second, pellet is resuspended by pipetting. After each of the two washings, the samples centrifuged again at 7500g and 4ºC for 5-10 minutes. Finally, the RNA samples are left to dry and then are dissolved in 20µl of DEPC water and stored at -80ºCin a freezer until further analyses.

To minimise freezing/thawing that will damage the RNA, once the RNA samples are resuspended in DEPC water, their quality/quantity is evaluated using NanoDrop™ ND-1000 spectrophotometer. The apparatus allows to measure RNA concentration measuring absorbance at 260nm. Moreover, the purity of the samples is assessed with use of two ratios: 260/280nm absorbance ratio, which gives information about DNA contamination in the sample and 260/230nm absorbance ratio, which provide information about any organic solvent contamination in the sample.

3.5.3 mRNA ANALYSIS BY RT-qPCR

The genes analysed in this study include *Plcb3* gene and other genes that are known to have a role on adipogenesis process such as *Pparγ2*, *Ap2*, *Cebpα*, *Srbp1c, Plin1, Plin2, in the de novo lipogenesis process i.e Fasn, Scd1 and in proliferation i,e Ki67*. Studying how, possibly, *Plcb3* gene silencing could affect the expression of these genes is important to unveiling the role of *Plcb3* in adipogenesis.

At first a retro transcription (RT) reaction is needed to convert the mRNA samples into complementary DNA (cDNA), which then, can be analysed by q-PCR. For the RT reaction, 0.5µg of mRNA is needed. 10µl of each sample containing 5µg of RNA are prepared by calculations based on the concentration's values obtained using 10µl of reaction mix, including reverse transcriptase i.e PrimeScript RT Master Mix (Takara Bio, San Jose, CA, USA). 0.5µg of mRNA is prepared by diluting the desired volume of RNA sample with DEPC water. Both 10µl of mix and samples are mixed on their respective PCR tube and transported on ice on to the thermocycler where RT reaction will occur using Takara program. The RT program starts with a step of 15 min at 37ºC followed by the RT enzyme inactivation step that raises temperatures up to 85ºC for 5s. Once enzyme is inactivated, a last incubation step at 4ºC is programmed allowing the preservation of cDNA samples until samples are taken.

Once the cDNA samples are collected, q-PCR protocol can start. First, 1:100 cDNA sample dilutions are prepared. Next, the forward and reverse primers for each gene analysed are added to the

reaction mix (SYBR Green) technology (TB Green: Takara Bio, San Jose, CA, USA). This mix contains a fluorescent DNA intercalator which binds new dsDNA molecules formed over each q-PCR cycle. The fluorescence of the DNA intercalator is generated by excitation at 496nm wavelength lasers and emission is detected at 520nm. Once samples and mix are prepared, 5µl of mix are firstly deposited in a well of a q-PCR 348-well plate and then 5µl of samples will be added. Once the wells are charged with both samples and mix, the plate is sealed with a cover to avoid evaporation and taken to the q-PCR machine, LightCycler 480 (Roche diagnostics, Basel, Switzerland). The amplification protocol consists of an initial preincubation step at 95ºC for 2 minutes. Then, each amplification round starts a 95ºC for 30s for denaturalization, then the temperature decreases to 60ºC for 30s for primer annealing and then there is a last step at 72ºC for 30s for elongation purposes. The amplification rounds are repeated for 45 cycles. After amplification, a melting temperature curve generated by increasing gradually the temperature from 60ºC to 97ºC at 0,11ºC/s to check for primers specificity. Finally, the samples are cooled at 40ºC for 40s after which they are maintained at 4ºC until collection.

For the samples analysis, the raw data are firstly ordered and processed into the right format using the LightCycler 480 software. After this, the CT values are obtained, which correspond to the PCR cycle in which the expression of the gene of interest is detected over the background noise. The CT results are then normalised two times. The first normalisation is done with respect to the housekeeping genes geometrical average (obtaining ΔCT). Analysed housekeeping genes include: 36b4, Rpl19, Ppia and B2m. A further normalisation is carried out normalising with non-target expression samples (obtaining ΔΔCT). Finally, to obtain expression values in fold change, Livak & Schmittgen´s formula is used:

- Livak and Schmittgen´s Fold change formula [1]:

$$FC = 2^{-\Delta\Delta CT}$$

3.6 Protein handling and analysis

3.6.1 Protein samples obtention and extraction

Protein samples are obtained from the cells seeded in the wells of the 12 well cell culture plate allocated to the different days of differentiation selected to be analysed. At first, we aspirate the medium and wash the well with 320 µl of PBS. Next, 50 µl of 1x RIPA (including: 50 mM Tris HCl, 150 mM NaCl, 1.0% NP-40, 0.5% Sodium Deoxycholate, 1.0 mM EDTA, 0.1% SDS and 0.01%, sodium azide at a pH of 7.4) are added to the cells and the whole well surface is scratched using the tip of the micropipette to detach all the cells. Then the cells resuspended in the RIPA buffer are transferred into a 1,5 ml tube, which is subsequently put in dry ice and stored at -80ºC.

For protein extraction, the samples are thawed by slowly on ice. The 1x RIPA buffer thin which the cells are already resuspended will lysate the cells. The samples are left to lysate for 30 minutes, during which we vortex the samples every 5 minutes. Next, the samples are centrifuged at 4ºC at maximum speed for 15-20 minutes. After the centrifugation, the supernatant (protein lysate) is collected and stored in the freezer at -20°C for further use.

3.6.2 Protein quantification using the Bradford protein assay

Before any further analysis, it is required to know the protein concentration. To measure it, we use a Bradford colorimetric assay (ThermoFisher Scientific, Walhtam, MA, USA). The colorimetric assay is carried out in a 96 well plate, where 200ul of Bradford reagent are transferred in every well to be used, keeping in mind that every protein sample collected will be measured in triplicates. Next, we set up BSA-based standard curve of increasing concentrations. Each point of the curve is loaded in triplicates. The standard curve includes the concentrations: 0, 0.125, 0.25, 0.5, 0.75, 1 and 1.5 mg/ml. We put 5µl of each concentration in each well. The BSA standard curve samples are prepared before the experiment by dilution of 2mg/ml stock of BSA in Miliq water. Next, 1µl of each sample is loaded in triplicates to its respective well of the 96 well plate. Once fully loaded, the plate is incubated for 10 minutes in the dark at room temperature. Finally, the colorimetry is measured at 595nm wavelength in a Perkin Elmer Wallac 1420 Victor2™ Microplate Reader apparatus (Perkin Elmer, Waltham, MA, USA).

3.6.3 PROTEIN ELECTROPHORESIS

Before immunoblot detection, the proteins in each sample need to be separated by their molecular weight. To do this, the samples are run on an SDS PAGE electrophoresis loaded in an Acrylamide 4-12% gradient gel *NuPAGE™* (ThermoFisher Scientific, Walhtam, MA, USA). Using the samples concentrations obtained previously by Bradford quantification, the protein amounts to be loaded for each sample are calculated to be 20µg of protein in 20µl of final sample volume. All samples must also include 5µl of Sample buffer NuPAGE LDS Sample Buffer 4X (4% SDS, 10% 2-mercaptoethanol, 20% glycerol, 0.004% bromophenol blue, 0.125 M Tris-HCl) (ThermoFisher Scientific, Walhtam, MA, USA) and 2µl of reducing agent 10X. The final volume of the sample will be increased to 20µl by addition of Miliq water. Once the samples are ready, they are incubated at 95ºC for 5 minutes, transfered to ice for 5 minutes and centrifuged at maximum speed for 1 minute. Next, the gel needs to be assembled into the electrophoresis cuvette XCell4 SurelockTM Midi-Cell (ThermoFisher Scientific, Walhtam, MA, USA) and the tank filled with MOPS (3-(N-morpholino) propanesulfonic acid) running buffer (MOPS free acid, Sodium Acetate, Disodium EDTA: ThermoFisher Scientific, Walhtam, MA, USA). Once the system is assembled 435µl of NuPAGE antioxidant (ThermoFisher Scientific, Walhtam, MA, USA) is added in the combs area. Next, the samples are loaded into their respective wells of the gel. Along with the samples, also a molecular weight i.e marker Spectra Multicolor Broad Range Protein Ladder (ThermoFisher Scientific, Walhtam, MA, USA) is loaded in the gel. The electrophoresis is run at 200V for 55 minutes.

3.6.4 BLOTTING AND IMMUNODETECTION

Before immunoblot detection, the protein samples separated on the acrylamid gradient gel are transferred onto a nitrocellulose membrane (ThermoFisher Scientific, Walhtam, MA, USA). The gel is maintained in a recipient covered by miliQ water while the transfer system is setup. The transfer is carried out using *aan iBlot™ 2 Gel Transfer Device* (ThermoFisher Scientific, Walhtam, MA, USA). Firstly, the gel is placed over *iBlot™ 2 Transfer Stack* (ThermoFisher Scientific, Walhtam, MA, USA), the bottom stack with the plastic tray having to be directly in contact with the transfer machine and the gel on top of the bottom stack. Next, the iBlotTM Filter Paper (ThermoFisher Scientific, Walhtam, MA, USA) is soaked in deionized water and put on top of gel. Then any possible air bubbles are removed by using the blotting roller unidirectionally over the filter paper. Furthermore, the top stack is added on top of the filter paper with the copper part facing up. At this stage, the

roller is used again to remove any bubbles formed. Finally, the iBlotTM 2 Absorbent Pad ThermoFisher Scientific, Walhtam, MA, USA) is added on top, aligning its conducting parts with the machine´s electrodes. Once the setup is done, the iBlot2 machine is closed and a transfer program is set at 25V for 7 minutes.

After the transfer is completed, the immunodetection takes place. For this, firstly, the nitrocellulose membrane is washed in PBS-T (PBS-Tween 20) and MiliQ water. Furthermore, the membrane is cut into separate parts according to sizes of the protein that we want to detect. The cutting of the membrane is carried out with the help of the molecular weight markers, scalpel tip and tweezers. Each membrane part is then blocked for 1h at room temperature on a roller mixer (Stuart, Stone, Staffordshire, UK) with 25ml of PBS-T 5% milk to avoid unspecific antibody binding. Next, the membranes are washed in PBS-T and incubated overnight on roller mixer at 4ºC with 5ml of their respective primary antibody diluted in PBS-T, 3% BSA. On the next day, the membranes are washed with PBS-T every 10 minutes for 30 minutes adding 20ml PBS-T every time and left on the roller mixer. After the washings, 5ml of secondary antibodies (Anti-mouse IGG, HRP-linked: Werfen, Barcelona, Spain; Anti-rabbit IGG, HRP-linked: Werfen, Barcelona, Spain), against mice or rabbit Ig, diluted in PBS-T 5% milk are added to membranes and left on a roller for incubation at room temperature for 1h. After incubation, more washes with PBS-T are carried out, every 10 minutes for 30 minutes and on a shaker. Furthermore, as the secondary antibody is conjugated with HRP (horse raddish peroxidase), for chemiluminescent detection, we incubated the membranes in the dark for 5 minutes with HRP substrate solutions. The substrate solutions consist of a mixture of 500µl of solution A (Solution A stock: 50ml contain 50 ul of Luminol solution, 220 ul coumaric acid solution, 5 ml Tris-HCl 1M, 44.73 ml of distilled water) and 500µl of solution B (Solution B stock: 50 ml contain 32 ul hydrogen peroxide, 5 ml Tris-HCl 1M, 44.97 ml of distilled water) mix (1:1). After incubation, the membranes are covered with plastic slips, removing any bubble formed and is transported to spectral fluorescence imaging system Alliance Q9 (Uvitec, Cambridge, Cambridgeshire, UK) for chemiluminescence detection of the protein signals.

3.6.5 Western Blot densitometric imaging analysis

Images obtained from luminescence captured by Alliance Q9 include bands of different intensity that represent the degrees of gene expression at protein level for the different samples. To objectively and empirically interpret the differences between band intensities, Image J image analysis software (Schneider et al., 2012) is used. Images are uploaded to the software, where rectangles are set to define an area in which all individual bands can fit. Then, measures of the average mean grey value are taken for every band and their close background. Once all samples and their background intensity are measured and named, ROI manager is used to save the data. A data table will be generated which includes mean grey values for every sample and background´s intensity values. In this way, a subjective band intensity difference has been turned into a numerical difference which can be normalised with its background and represented.

3.7 Lipid droplet staining and immunofluorescence

In order to carry out a morphological analysis of the adipocytes at the different days of differentiation, the cells were fixed and stained with later explained reagents. For that, cells were seeded in the wells of the culture plate on round coverslips.

Before staining, cells are fixed. The fixation ensures that the cells stop replicating and differentiating. and keep their morphological structural features, allowing to “freeze time” and study the cells at each moment of their differentiation cycle. Before the cells are fixed, the medium is removed, and the cells are washed twice with 500µl of PBS per well. Furthermore, the fixation takes place by adding 500µl of paraformaldehyde (PFA) 4% (ThermoFisher Scientific, Walhtam, MA, USA) in each well and left to incubate at room temperature for 15 minutes. After incubation, the PFA is removed and the cells are washed three times with 500µl of PBS. Finally, 2ml of PBS are added into each well and the plate is sealed with parafilm and stored at 4ºC until cell staining.

To allow the cell staining reagents and antibodies to reach their intracellular target, the fixed cells are permeabilised. The permeabilization is carried out by adding 500µl of permeabilization solution, consisting of 0,1% TrittonX-100 in PBS 1X, to each well containing the coverslip and by incubating them at room temperature for 10 minutes. After incubation, another three PBS washings are carried out.

Following the permeabilization, a blocking step takes place. The blocking ensures that, later, the antibodies used to mark the intracellular components bind to specific targets. So, 500µl of blocking solution including 2% BSA in PBS 1X are added on each well. The wells with the blocking solution are incubated at room temperature for a minimum of 30 minutes.

Once the cells are fixed, permeabilised and blocked, staining reagents and antibodies can be applied. Firstly, the incubation with primary antibodies is carried out. The primary antibody is prepared in blocking solution (2% BSA in PBS 1X). *PLIN1* antibody is diluted 1:200 in blocking solution. Once the primary antibody in the blocking solution is prepared, 100µl of it are added on each well and left to incubate at 4ºC in high humidity overnight. On the next day, three washings with 1ml PBS are carried out. The secondary antibody (Rb647) is prepared is diluted in the blocking solution 1:500. The secondary antibody is also prepared with the fluorescence marking reagent *LipidTOX™ Red staining* (ThermoFisher Scientific, Walhtam, MA, USA) in a 1:200 dilution. LipidTOX stains the lipid content of the lipid droplets. Once prepared, 100µl of secondary antibody and fluorescent reagent solution are added to each well and it is incubated at room temperature for an hour. After incubation, the secondary antibody solution is removed and 500µl of a solution of 1:1000 of *DAPI working solution* (4’,6-Diamidine-2’-phenylindole dihydrochloride: Sigma-Aldrich, St. Louis, MO, USA) diluted in PBS is added on each well and incubated for 10 minutes. After incubation, each coverslip is washed individually by carefully picking them up with tweezers and dipping three times each coverslip in PBS, MiliQ water and finally on PBS again. After washing, the coverslips are gently dried by tapping them on paper.

To prepare the samples for microscopy, two 20µl drops of *Fluoromount™* (Sigma-Aldrich, St. Louis, MO, USA) mounting medium are placed on each slide. Next, the coverslips with the stained cells are turned upside down, so that cells are in contact with the mounting medium fluoromount drops. We normally fit two coverslips per slide, one over each mounting medium drop. The slides are then left to dry in the dark. Once dried, the mounted slides can be kept at 4ºC until the confocal microscope analysis for immunofluorescence imaging is carried out. DAPI´s emission is detected at

340/488nm and LipidTOX´s emission is detected at 577/609nm. For the secondary antibodies, *PLIN* 1 is detected at around 488nm.

3.8 STATISTICAL ANALYSIS

For the statistical analysis of the results, the arithmetic mean was taken as a measure of the main trend and the standard deviation (SD) was taken as a measure of dispersion. Since these were independent samples and did not present normality (nonparametric) due to the low n, the Kruskal-Wallis test was applied ("Kruskal-Wallis Test", 2008), which allows the comparison between the different groups. The sample size used in each subgroup for analytical determination was n=3, statistical differences were assumed when the p-value of the appropriate comparison test was below 0.05.

4. RESULTS

4.1 BIOINFORMATIC ANALYSIS

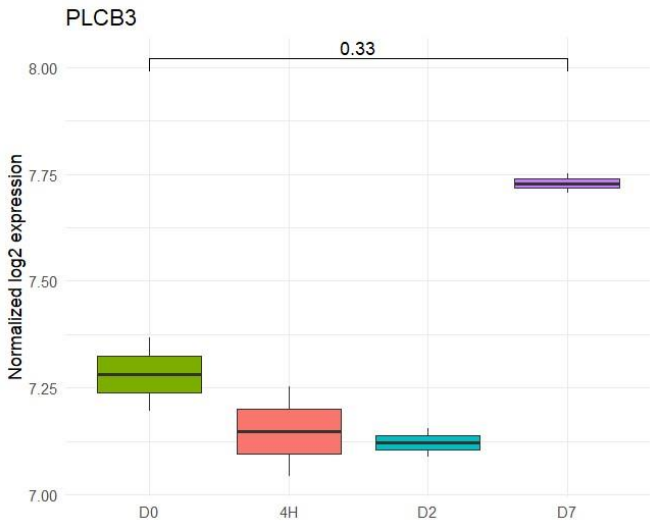

Figure 7: Bioinformatic analysis boxplot for Plcb3 expression on 3T3-L1 over adipogenesis: gene expression was measured for day 0 (D0), 4 hours (4H), day 2 (D2) and day seven (D7) of differentiation). Image extracted from a previous study done by Rasmus Siersbæk et al (2016)

We preliminarily profiled the expression of the *Plcb3* gene by performing bioinformatic analysis of the GSE95533 dataset (RNA-seq of murine 3T3-L1 preadipocytes) from the GEO public repository (33). As illustrated in Figure 7 the expression of *Plcb3* gene appears to peak at day 7 of differentiation, this suggests that *Plcb3* expresses during the latest days of adipocyte differentiation and therefore it could be potentially participating in the process. Expression of *Plcb3* at Day 0, 4H and D2 is significantly lower than at Day 7, in addition to this, their standard error bars overlap, meaning that they have a similar expression pattern that is different from the one at Day 7.

4.2 MOI ASSAY RESULTS

In order to study the role of *Plcb3* in the adipogenesis of the 3T3L1 murine adipocyte cell line, we generated a *Plcb3* knockdown 3T3-L1 cell line. For this, we decided to use a lentiviral approach to silence its expression and test which are the effects of the deficiency of this gene in adipogenesis progression. We treated 3T3L1 preadipocytes with different MOI of the lentivirus carrying a *Plcb3* shRNA. We validated *Plcb3* mRNA and protein levels at the different MOI of lentivirus used, by qPCR and WB. This experiment was only done with one replica, hence the lack of standard error bars in figures 8 and 9.

The results of the % of *Plcb3* mRNA silencing for the 3 MOIs concentrations (MOI3, MOI 5 and MOI 10) are displayed on Figure 8. In this figure, it is shown that the MOI5 is the lentiviral concentration which has greater impact on *Plcb3´*s mRNA expression with respect to the MOI´s 3 or 10. It is also interesting to comment that although the MOI 10 has the greater lentiviral concentration, it shows the smallest silencing %, being 38% less than the MOI5 and 15% less than the MOI3.

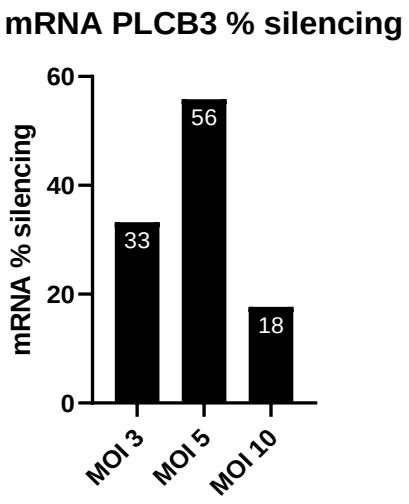

Figure 8: Percentage of *PLCB3* mRNA silencing for each of the used MOI (multiplicity of infection) of lentivirus. Each column has its exact percentage of silencing marked in white

To validate the mRNA results of the silencing, *PLCB3* protein expression levels were also measured for each MOI. The results shown in Figure 9, illustrate how MOI´s 3 and 5 present similar % of *PLCB3* protein silencing, being greater than MOI 10. From both mRNA and protein MOI results (Figures 8 and 9), the MOI 5 appears to have the greatest % silencing on both protein and mRNA expression. Even though MOI3 has similar silencing on protein expression it was discarded for its low silencing on mRNA.

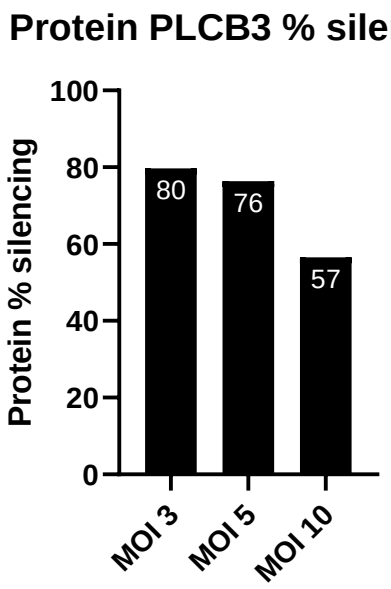

Figure 9: Percentage of PLCB3 protein silencing for each of the used MOI (multiplicity of infection) of lentivirus. Each column has its exact percentage of silencing marked in white

4.3 PLCB3 EXPRESSION PROFILE UNDER WILD TYPE CONDITIONS

To better characterize the role of *Plcb3* gene in adipogenesis, a differentiation experiment is done comparing the mRNA and protein expression over the 9 days of differentiation for both silenced and non-silenced 3T3-L1 cells. The mRNA and protein expression profile of the gene was analysed for silenced (*Plcb3* group) and non-silenced cells (non-target NT cells).

4.3.1 MRNA EXPRESSION PROFILE OF PLCB3

Figure 10.A shows how *Plcb3* gene expression varied during differentiation. We observed how gene expression showed lower levels during the initial days (D0-D3) of differentiation and then, the expression peaks at day 5, after which, it gradually decreases back to its basal level of expression. Whereas the mRNA expression of the non-target group varies with time, the silenced group (*Plcb3* group) had a rather constant expression throughout the differentiation process.

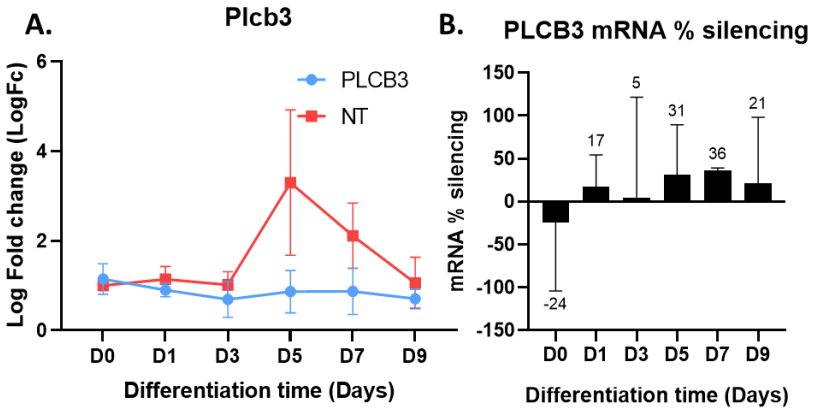

Figure 10: *Plcb3* mRNA gene expression silencing levels during 3T3L1 adipocyte differentiation. A: Graph of mRNA expression of *Plcb3* (Log Fold Change) at different days of differentiation for conditions *Plcb3* (silenced) and NT (non-target). B: Bar graph of *Plcb3* mRNA silencing in % for each day of differentiation, individual mean %silencing values

are located above de standard error bar of each sample. The graphs in Figure 10.A and 10.B include standard error bars associated to each value obtained from all four replicates.

4.3.2 Protein expression profile of PLCB3

In order to validate mRNA expression result, we analyzed the protein expression profile of *PLCB3* during differentiation for the *PLCB3* silenced and NT groups, what is shown in Figure 11.A. The protein expression pattern for *PLCB3* followed a similar trend the one seen in Figure 10.A for the mRNA. However, *PLCB3* protein expression appeared to be shifted to earlier days, since the peak expression was now at Day 3 instead of Day 5. As expected, *PLCB3* protein expression for the silenced group appeared to decrease over time. In Figure 11.B, the % of *PLCB3* silencing appeared to be more robust during adipogenesis than in Figure 10.B. We could highlight days 7 and 9 of differentiation for having a % silencing close to 70%, as well as days 0 and 3 for having a silencing close to 30%.

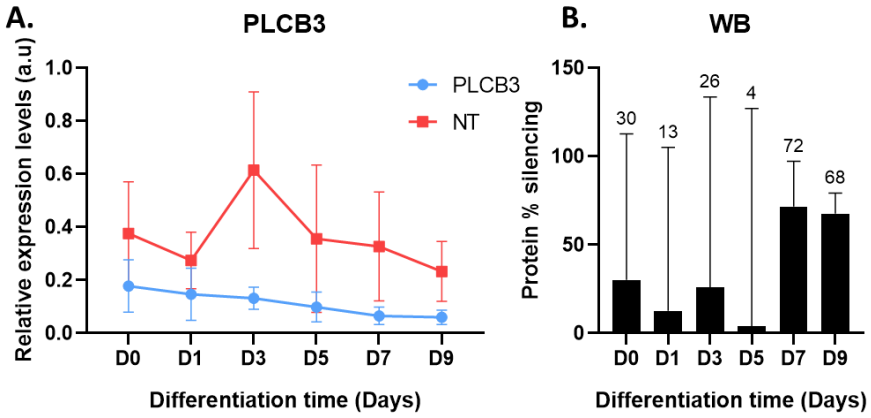

Figure 11: *PLCB3* protein expression silencing levels during 3T3L1 adipocyte differentiation. A: Graph of protein expression of *PLCB3* (Log Fold Change) vs at different days of differentiation for conditions *Plcb3* (silenced) and NT (non-target). B: Bar graph of *PLCB3* protein silencing in % for each day of differentiation, individual mean % silencing values are located above de standard error bar of each sample. The graphs in figure 11.A and 11.B includes standard error bars associated to each value obtained from all four replicates.

4.4 Effect of PLCB3 silencing on key adipogenesis genes

Once we analyzed the mRNA and protein expression profile for *Plcb3* gene, the next step was to look at the effect of its silencing on key adipogenesis genes. The analyzed genes were divided into four main categories: markers of early differentiation genes (*Pparγ* ISO1/2 and *Cebpα*), lipid droplet formation marker genes (*Plin1* and *Plin2*), *de novo* lipogenesis genes (*Fasn*, *Srebp1c* and *Scd1*) and proliferation marker (*Ki67*). Each set of genes was analyzed for its mRNA and protein expression levels.

4.4.1 mRNA analysis

As mentioned earlier, *PPARγ2* and *CEBPα* are key genes involved in early adipocyte differentiation. In figure 12.A, *PPARγ2* expression profile displayed, for the silenced group, a tendency to be

increased at days 3 and 5 of differentiation vs the NT group, whereas in later days of differentiation it showed a downregulated mRNA expression level for the same experimental group vs NT controls. *PPARγ2* also appeared to show its expected expression pattern for both experimental groups. Finally, *Cebpα* appeared to have a similar profile of expression (Figure 12.B) between both groups except for days 3, 7 and 9. We could see that for the *Plcb3* group *Cebpα* is upregulated with respect to NT group at days 3 and 7, whereas its expression at Day 9 is increased, for NT group's indicating a tendency to be downregulated for *Plcb3* group at Day 9.

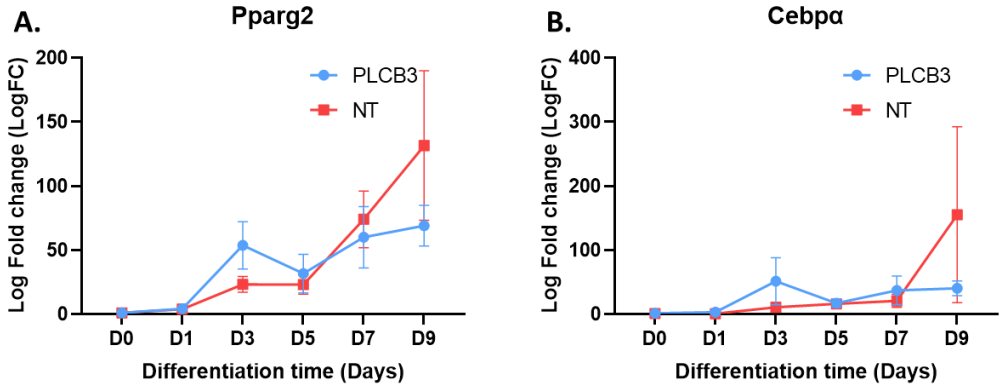

Figure12: mRNA expression of early markers of adipogenesis. A: mRNA expression (LogFC) at different days of differentiation for *Ppary* B: mRNA expression (LogFC) with at different days of differentiation for CEBPα. All graphs include standard error bars associated to each value obtained from all four replicates.

For makers of lipid droplet formation and late adipogenesis, which are highly expressed on the late stages of differentiation, we looked at the expression levels of *Plin1*, *Plin2 and Ap2,* respectively. Figure 13.A, showed a clear tendency of downregulation of *Plin1* for the silenced group, whereas of the NT group, its expression showed the expected expression pattern, displaying a peak of expression at days 7 and 9 of differentiation. Even though, for the *Plcb3* group *Plin1* expression slightly increased at day 3, for the rest of the differentiation time course its expression remained at a constant low level. *Plin2* (Figure 13.B) also shows a similar tendency to be downregulated at days 7 and 9 for the *Plcb3* group vs NT controls. Figure 13.C shows how AP2 appears to show its normal expression pattern in adipogenesis, showing no expression during the first days (D0-D3) as it only acts during the later days of differentiation.

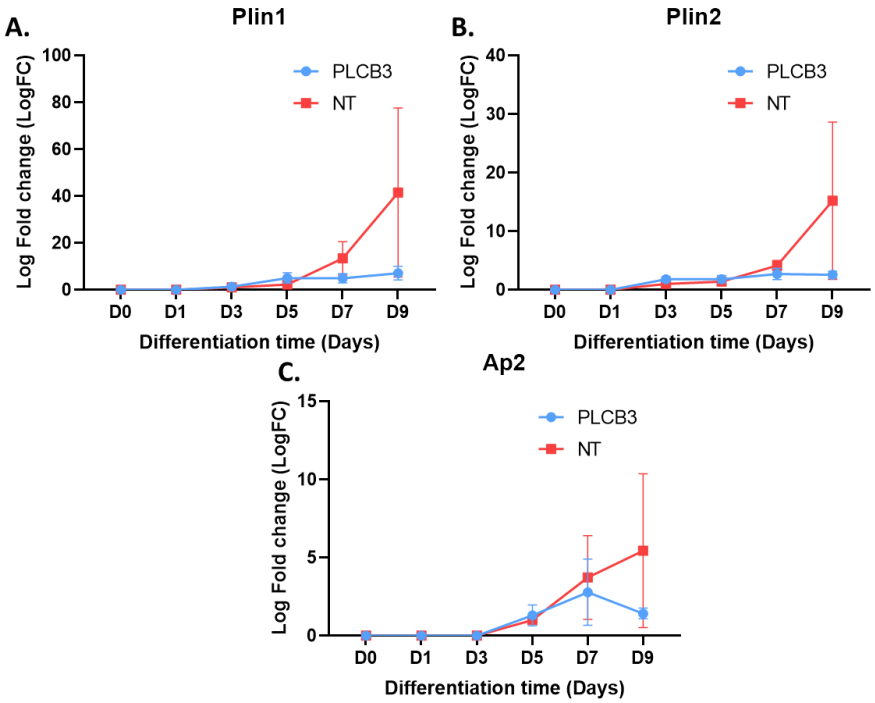

Figure 13: mRNA expression levels of late markers of adipogenesis. A: mRNA expression (LogFC) at different days of differentiation for *Plin1*. B: mRNA expression (LogFC) at different days of differentiation for *Plin2*. All graphs include standard error bars associated to each value obtained from all four replicates.

Concerning the markers for the *de novo* lipogenesis (*Fasn*, *Srbp1c* and *Scd1*), all appeared to show similar mRNA expression patterns between the two experimental groups. *Fasn* (Figure 14.A) was slightly upregulated in the *Plcb3* vs the NT group during differentiation. *Srbp1c* results (Figure 14.B) appeared to show a tendency to an upregulation for *Plcb3* silenced group vs controls. However, at day 7 of differentiation, in the NT group increased drastically above *Plcb3* group, then its expression, at Day 9, lowered back to below *Plcb3* expression. For *Scd1* (Figure 14.C) both experimental conditions seemed to have a very similar expression profiles, having only two days where expression was slightly diverted amongst them (Day 3 and Day 9).

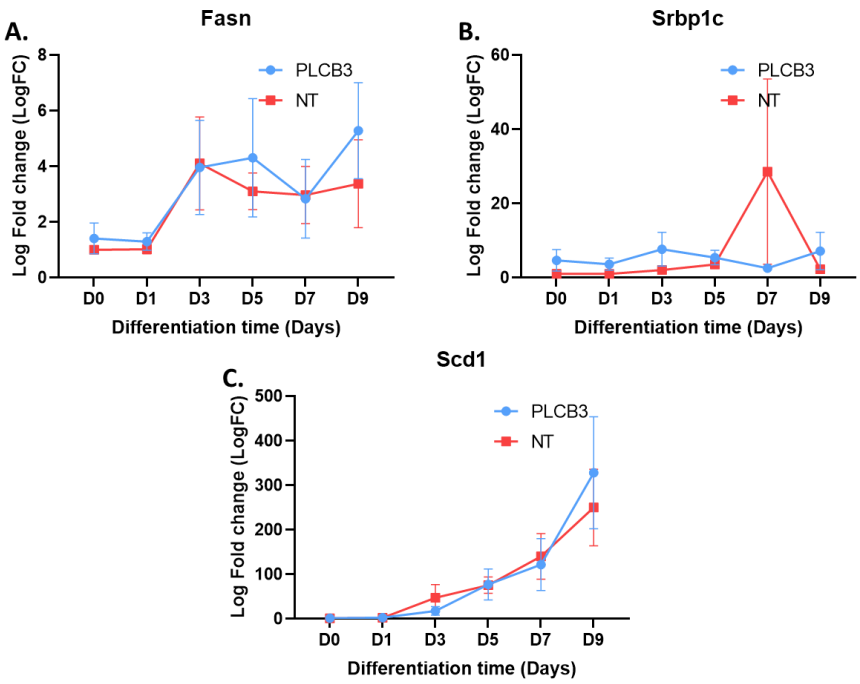

Figure14: mRNA expression levels of *de novo* lipogenesis genes. A: mRNA expression (LogFC) at different days of differentiation for *Fasn*. B: mRNA expression (LogFC) at different days of differentiation for *Srbp1c*. C: mRNA expression (LogFC) at different days of differentiation for *Scd1*. All graphs include standard error bars associated to each value obtained from all four replicates.

To assess potential differences in proliferation between the *Plcb3* and NT groups we analyzed the expression levels of *Ki67*, a well-known proliferation marker. Its expression showed a tendency to be upregulated in the *Plcb3* group with respect to NT group, for most of the days, except for Day 7 (Figure.15), in which it seemed to be slightly more expressed in the NT group. Ki67 expression results showed an expected pattern, as we can see that the peak of expression lies on the first day of differentiation (Figure.15), when the cells undergo mitotic clonal expansion.

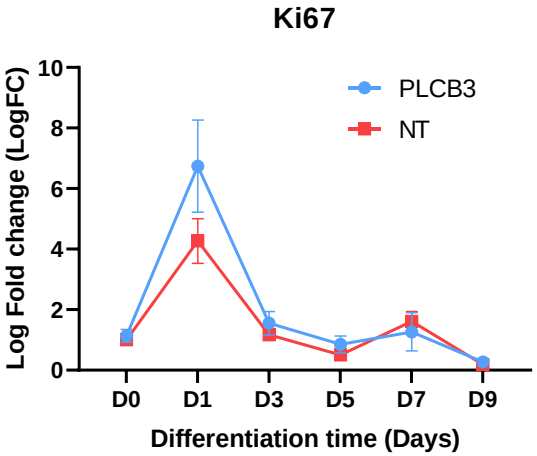

Figure 15: mRNA expression (LogFC) for the proliferation marker *Ki67 at different days of differentiation for the Plcb3 and NT experimental groups. This graph includes standard error bars associated to each value obtained from all four replicates.*

4.4.2 Protein analysis

Protein expression analysis were then carried out to validate the changes seen in mRNA expression. Firstly, we confirmed that *Plcb3* gene was silenced in *Plcb3* group (Black) when compared to the NT group (Blue) as it can be observed in Figure 16.

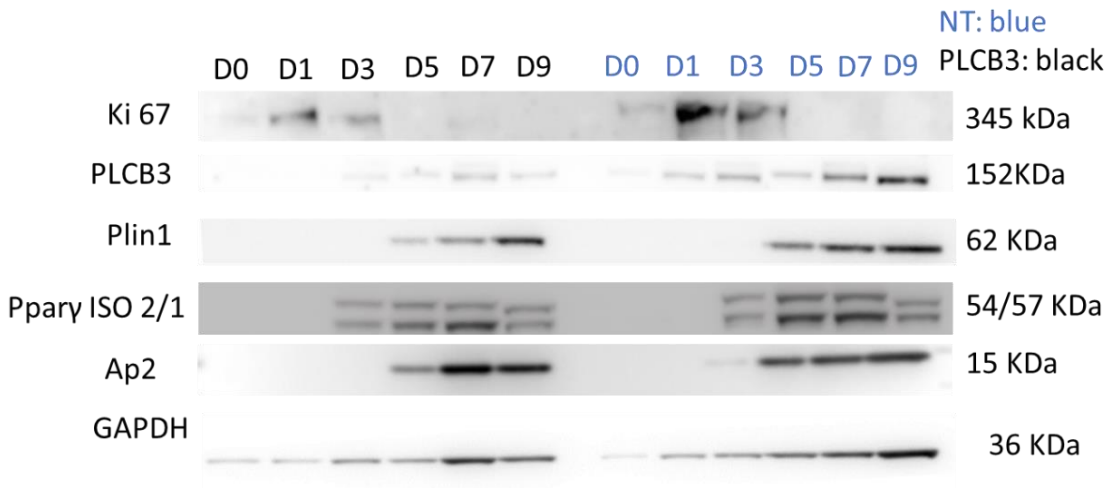

Figure 16: Immunoblot analysis of PLCB·, the adipogenic genes *PLIN1*, *PPARγ ISO1/2*, and *AP2* and the proliferation gene *Ki67*. The Western blot images show the samples divided in 2 groups: silenced group (*Plcb3*, black) and non-target group (NT), blue. The images of the wb bands showed here have been selected as they are representative of the results obtained from a n=4 replicates.

To validate the results obtained with mRNA analysis, a protein analysis by western blot taked place. For protein analysis we checked the expression of two adipogenesis markers: *PPARγ* and *Ap2.* With the same primary antibody, we were able to detect both isoforms for *PPARγ* protein, i.e *PPARγ 1* and *2,* for which their immunoblot results are included in figure 17.A and figure 17. B. For the first isoform of *PPARγ* (ISO1) (Fig 17.A), there were no differences in its protein expression levels between *Plcb3* group and the NT group. For the second isoform of *PPARγ* (ISO2). In Figure 17.B, we could observe a tendency to an upregulation for the *Plcb3* group with the exception of day 3, in which the NT group showed a higher expression of this protein. The protein expression pattern for *PPARγ* ISO2 fits with what was expected for the expression of this gene, as it had its peak expression at day 3. *AP2* protein expression (Fig17.C) matched what's observed for the mRNA expression (fig12.A) for the *Plcb3* group, with the exception of day 5, where we observed an upregulation for the NT group not seen in the mRNA expression analysis (fig 12.A). *AP2* results in Figure 17.C also matched the normal expected expression profile for the gene, as *Ap2* is only expressed normally from days 5 to 9 of differentiation.

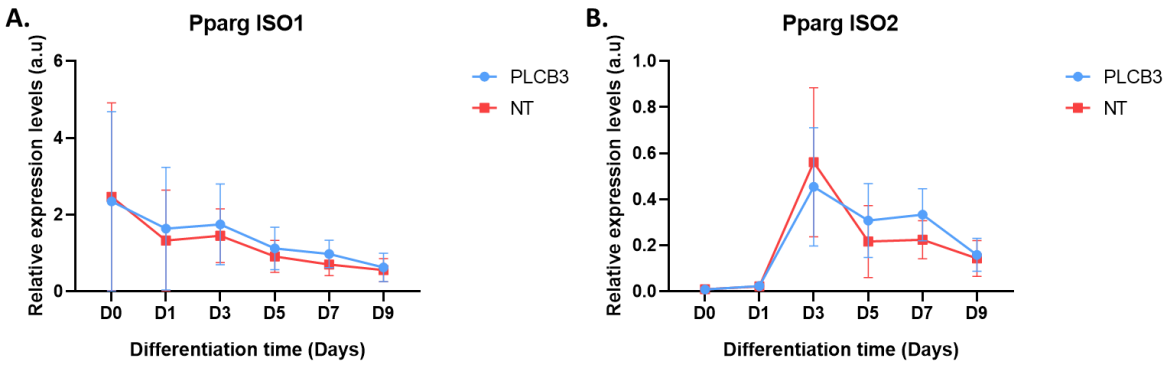

Figure 17: Protein expression for the adipogenesis markers *Pparγ* and *AP2*). A: Protein expression (Relative expression) at different days of differentiation for *PPARγ* isoform 1. B: Protein expression (Relative expression) at different days of differentiation for *PPARγ* isoform 2. C: Protein expression (Relative expression) at different days of differentiation for *AP2*. All graphs include standard error bars associated to each value obtained from all four replicates.

The protein expression results obtained for the late adipogenesis markers *PLIN1* (Figure 18) are similar to the results showed in figure 13.A. At days 7 and 9 the NT group expressed more *PLIN1* protein than the silenced group. However, at day 5, *PLIN1* protein levels appeared to be upregulated for the *Plcb3* group. The protein expression profile for the *Plcb3* group started earlier and it was maintained at a lower level throughout differentiation when compared to the NT group. Regarding the NT group, it seemed that the peak of expression for *PLIN1* is day 7, instead of day 9 of differentiation.

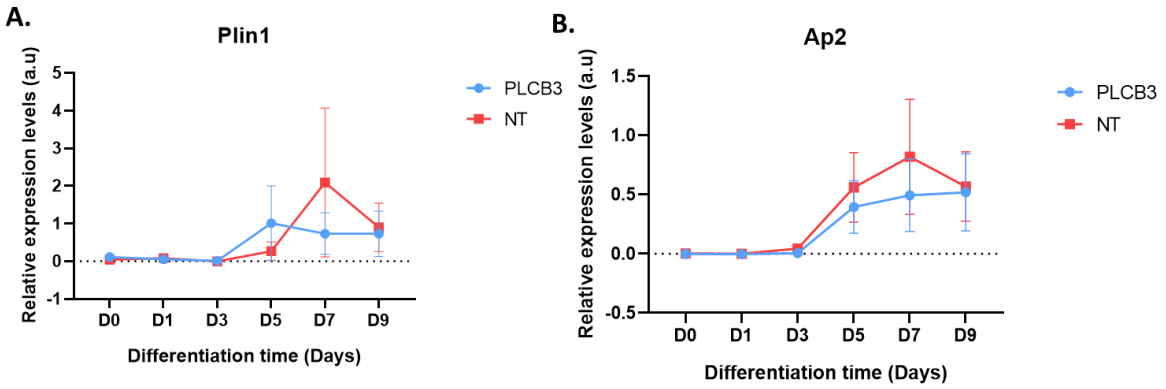

Figure 18: Protein expression of late markers of adipogenesis, *PLIN1*. *Its expression has been analysed comparing the results of the NT and the Plcb3 groups at different days of differentiation. This graph includes standard error bars associated to each value obtained from all four replicates.*

Regarding the protein expression levels of the proliferation marker *KI67*. Its protein expression (figure 19) levels seemed to be opposite from those seen in figure 15 for Ki67´s mRNA expression. In figure 19, *KI67* seemed to be upregulated in the NT group and not in the *Plcb3* group as shown in figure 15. Once again, the expression profile of *Ki67* for both experimental groups matched what was expected normally for an adipocyte, i.e., the maximum expression level of *Ki67* at day 1 and then have very low/zero expression in the later days of differentiation.

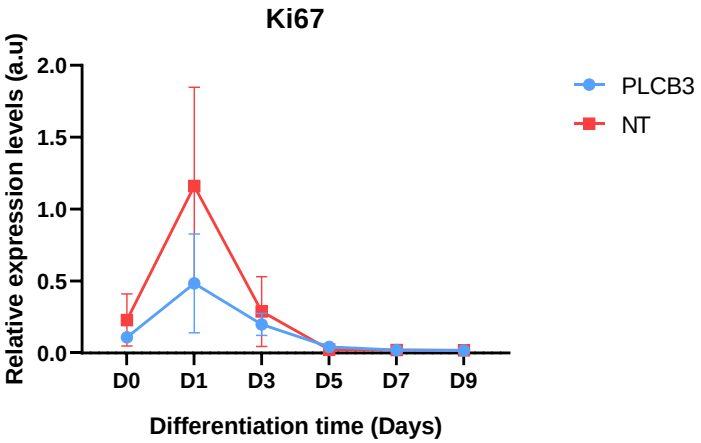

Figure 19: Protein expression for the proliferation marks, *KI67* in both groups (NT and *Plcb3*) at different days of differentiation. This graph includes standard error bars associated to each value obtained from all four replicates.

4.4.3 IMMUNOFLUORESCENCE MORPHOLOGICAL ANALYSIS

Finally, we performed morphological analysis to confirm if earlier mRNA and protein expression results are translated into visible adipocyte morphological differences during differentiation and proliferation. This analysis is focused on the expression of late adipogenesis neutral lipids staining with LipidTox (Red) at Day 3 to Day 9 as well as PLIN1 lipid droplet formation protein immunostaining for days 3-9 and *Ki67* Proliferation protein immunolabelling for day 1.

Regarding proliferation, *KI67* immuno labeling was performed on in Day 1 slides. *KI67* is labelled in green color, although, as its expression is in the nucleus, it overlaps with DAPI´s blue staining. As a result, the cells expressing *KI67* will show a cyan/light blue colored nucleus. By comparing Day 1 images of figures 20 and 21, we could see that for the *Plcb3* group (figure 21) there seemed to be a higher number of nuclei stained and they seemed to have a greater intensity than for the NT group. These results were consistent with the results obtained with the mRNA analysis (figure 15), and it shows that *KI67* gene had been upregulated in the silenced group.

Regarding *PLIN1* labelling, it is present at days 3-9 and it is marked in green color. *PLIN1* expression is only visible from days 7 to 9 for both conditions (Figures 20 and 21), what correlates with the expression profile observed with the mRNA analysis (Figure 13). Furthermore, PLIN1 in both figures 20 and 21 seemed to be expressed, as expected, in the periphery of lipid droplets, surrounding the red lipid labeling. In addition to this, PLIN1 seemed to be upregulated in NT condition at day 7 and very slightly downregulated at day 9. These results matched those seen for the protein analysis (Figure 18) and the ones of mRNA analysis only for day 7 (Figure 13).

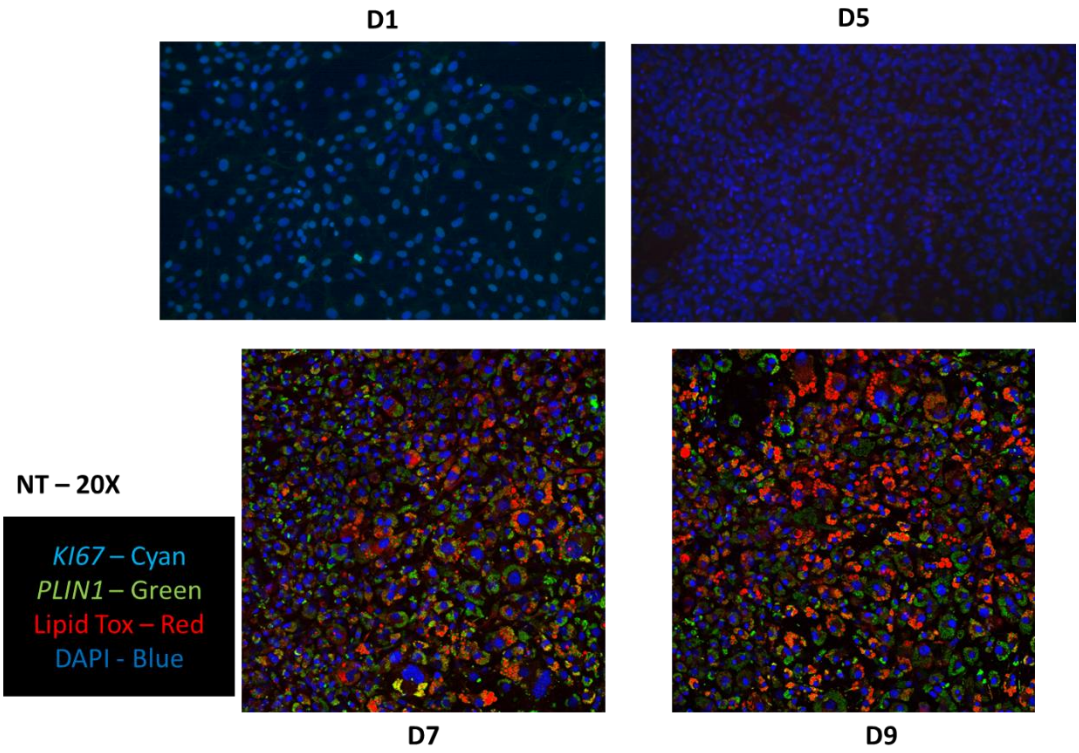

Figure 20: Morphological analysis by immunofluorescence for the NT condition. Day 1 image has *KI67* marking in green color, although it is seen as light blue as it overlaps with DAPI at the nucleus. For Days 3-9, nucleus is marked on blue with DAPI, lipid droplets stained with LipidTox are marked on red and *PLIN1* is marked on green. All images have been taken using 20x lens. Images shown have been extracted from fourth replicates, for their good representation of global immunofluorescence results and their good image quality. Days 7 and 9 images have been taken with confocal microscopy, whilst days 1-5 have been taken using Dcim8 fluorescence microscope.

Concerning the neutral lipid staining with LipidTox (seen in red), when comparing day 7 and 9, for both conditions (Figures 20 and 21), the lipid droplet morphology seemed to be similar on both conditions, although at Day 7 for *Plcb3* condition the sized lipid droplets appeared to be smaller. At day 9, the results could indicate that the NT condition (figure 20) shows a higher number of lipid droplet development than *Plcb3* condition. These results were consistent with the mRNA analysis results shown in figures 12 and 13 as well as those seen in protein analysis (figures 17 and 18) in which most adipogenesis genes appeared to be slightly downregulated for days 7 and 9, with the exception of *Pparγ2* ISO 1/2 (figure 17), which appeared to be slightly upregulated in *Plcb3* group.

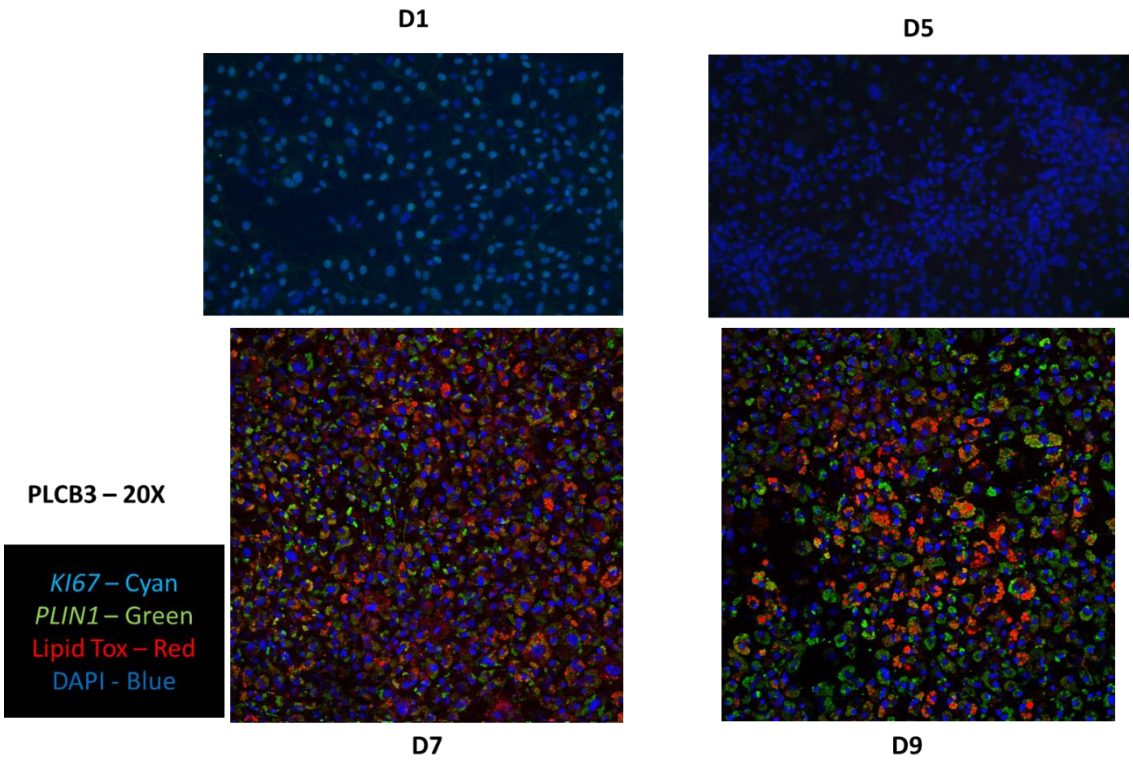

Figure 21: Immunofluorescence morphological analysis results for Plcb3 condition. Day 1 image shows *KI67* marked in green color, although it is seen as light blue as it overlaps with DAPI at the nucleus. For Days 3-9, nucleus is marked on blue with DAPI, lipid droplets stained with LipidTox are marked in red and *PLIN1* is marked in green. All images have been taken using 20x lens. Images shown have been extracted from fourth replica, for their good representation of global immunofluorescence results and their good image quality. Days 7 and 9 images have been taken with confocal microscopy, whilst days 31-5 have been taken using Dcim8 fluorescence microscope.

5. DISCUSSION

As commented earlier (section 1.3), the selection of *Plcb3* gene for this project comes from a GWAS which related it with a metabolically healthy obese (MHO) phenotype. Being MHO individuals characterized by having a high BMI (BMI > 30) whilst not suffering of any obesity related comorbidity. Plcb3 gene has specifically been grouped into the MHO phenotype for its statistically significant relationship with higher HDL cholesterol levels, low triglyceride levels whilst still promoting fat development (23). Although *Plcb3* has been classified as leading to an MHO, the mechanism is still unknown of how the gene contributes to creating this phenotype by promoting fat development and decreasing risk of obesity related comorbidities.

For these reasons, it has been decided to investigate the expression profile of *Plcb3* during adipogenesis which could potentially help to discover the role of *Plcb3* in adipogenesis. To achieve this, an initial bioinformatic analysis is done showing with statistical relevance how *Plcb3* has a peak of expression at day 7 of differentiation, however this doesn't mean *Plcb3´*s actual peak expression is at day 7, as days between Day 2 and Day 7 or days higher than Day 7 are not included in the

analysis. Therefore, to better characterize *Plcb3´*s expression profile, we will need to rely on mRNA and protein analysis. But as a preliminary result, it does prove that the studied gene increases it expression during adipogenesis suggesting a potential role in this process.

Secondly, a silencing MOI pilot assay takes place in order to validate the degree to which the transfected 3T3-L1 cells have been silenced for *Plcb3* gene. The silencing was done using lentivirus, as this molecular biology technology allows for a more stable silencing of the gene of interest with time (34), as silencing needs to be as stable as possible throughout the 9 days of differentiation. In addition to this, the decision to use lentiviral silencing was reinforced by the fact that, as it was found in previous experiments done by our lab that silencing using siRNA was not stable for the 9 days of differentiation. The MOI assay results (section 4.2) show how MOI´s 3 and 5 have greater silencing than MOI 10. A possible explanation to this effect is that when the viral concentration is too high, the cytotoxic effects (35) of the virus affect negatively the gene expression, as perhaps, the increased viral titer could be altering normal cell expression. The fact that MOI 5 has a higher mRNA silencing and a similar protein silencing to that of the MOI 3, made MOI 5 the best candidate.

Once selected the MOI 5 and generated the stable *Plcb3* silenced cell line, we performed the differentiation for 9 days following the mentioned protocol. After this, mRNA and protein expression analysis took place. From these results we investigated three important aspects: *Plcb3* normal expression patter validation, effect of *Plcb3 silencing* on early and late adipogenesis genes, and the effect of *Plcb3 silencing* on adipocytes proliferation. Regarding the validation of *Plcb3´*s normal expression profile (section 4.3.1), the gene appears to have a peak of expression between days 3-5 of differentiation. This could mean that, if *Plcb3* does affect adipogenesis, it would be on early stage adipogenic gene expression such as on the expression of *Cebpα,* which is one of the first genes to be activated in adipogenesis and acts activating expression of Pparγ key adipogenesis regulator (9). The results also confirm that effectively *Plcb3* was silenced in the *Plcb3* condition during the differentiation process. However, unfortunately the % of silencing for the gene seems to not be robust throughout the differentiation process, except for final days of differentiation. One possible explanation for this would be the fact that Plcb´3s expression on the first days of differentiation is very low, making the silencing less obvious between conditions. Existing bibliographic evidence (36) suggested how *Plcb1*, one of the four isoforms of the *Plcb* gene family, that also produces DAG and IP3 as result of its activity, has been shown to play a role in early days of differentiation in 3T3-L1 mouse preadipocyte cells. This interesting research information could possibly point towards *Plcb3* gene also having a role in early stages of adipogenesis. This evidence is therefore in line with *Plcb3* gene having a peak expression on earlier days of differentiation such as Day 3 or 5 and could also point towards the gene having a role in the regulation of early adipogenesis genes expression.

Following those experimental results, the next step was to analyze the effect of *Plcb3* silencing on key adipogenesis genes. For this, mRNA and protein expression for relevant adipogenesis markers was measured for both NT and *Plcb3* conditions. Regarding the mRNA and protein expression results for early adipogenesis genes (*Pparγ2*, *Cebpα*), these suggest how *Plcb3* silencing could have caused a slight increase in early adipogenesis expression genes, with the exception of Cebpα and Pparγ2 for later days 7 and 9. These results could point towards the hypothesis that *Plcb3* expression could affect slightly downregulating early adipogenesis process. Moreover, the fact that *PPARγ* protein expression is similar in both conditions might mean that the effect of *Plcb3* in

adipogenesis occurs after *Pparγ* signaling on the adipogenesis process, as *Pparγ* is the key master regulator of adipogenesis which initiates the gene expression cascade in adipogenesis (8). Regarding late adipogenesis expression genes (*Plin1* and *Plin2*) there appears to be an upregulation tendency in both protein and mRNA expression. This reinforces the earlier mentioned hypothesis that *Plcb3* could contribute to adipogenesis process. There is research evidence prior to this project which suggests that one of the products of *Plcb3* enzymatic activity, DAG can activate Protein kinase C delta isoform (PKC-δ). This isoform of PKC has been shown to affect differentiation in 3T3-L1 cells by lowering expression of early adipogenesis genes such as *Pparγ* and *Cebpα* (37). This bibliographical evidence could possibly explain why *Pparγ* and *Cebpα* were upregulated in the earlier days of differentiation with respect to mRNA and protein expression in the silenced group.

Next, the effect of *Plcb3* silencing on late adipogenesis genes was also analyzed at both mRNA and protein expression levels. Surprisingly, the results appear to point towards the silencing having a downregulation effect on late adipogenesis genes, which is opposite effect of what was seen in early adipogenesis genes. Previous research on the effect of calcium on adipogenesis seems to support this hypothesis. As commented in section 1.6, *PLCB3* is a membrane bound phospholipase which forms IP3 from PIP2, this IP3 then acts intracellularly opening endoplasmic reticulum calcium channels and increasing cytosolic levels of calcium. The effect of calcium on adipogenesis has been previously deeply characterized in bibliography and can be contradictory if not studied more in depth. For instance, high levels of calcium would activate AMPK pathway via calcium/calmodulin dependent kinase (CAMKK2). CAMKK2 is known for inhibiting adipocyte differentiation via inhibition of early adipogenesis genes such as *Cebpα* (38). Cebpα and Pparγ early adipogenesis genes have effect over late adipogenesis genes, as they trigger the signaling cascades that regulate their expression (9). However previous studies show that AMPK is not as relevant in mice adipose tissue differentiation as it is for human adipose tissue (39). Another way in which Calcium could affect adipogenesis is via the calcium sensing receptor (CaSR), bibliographical studies done with this receptor show how it does promote adipogenesis by promoting the expression of Pparγ signaling pathway (40). These could explain why most adipogenesis genes seem to be downregulated in the *Plcb3* condition, because *Plcb3* is normally acting as an adipogenesis promoter via CaSR receptor amongst other possible mechanisms.

Another key pathway that participates in the fat accumulation in adipocytes is the *de novo* lipogenesis. The *de-novo* lipogenesis process involves the formation of fatty acid chains from acetyl Co-A produced in glycolysis (41), this mechanism functions primarily in conditions of low-fat intake or excess carbohydrate intake. DNL was especially interesting as it allows us to control the other possible way in which adipocytes can synthetize lipids apart from conventional. For *de-novo* lipogenesis genes (*Fasn*, *Srbp1c*, *Scd1*) mRNA expression we can observe how, unfortunately, results for all three genes are very close for both groups, meaning that the standard error bars overlap almost completely. On top of this, the expression profiles for Fasn and Srbp1c genes for the non-target group appear to be different from expected one, as they should show an expression pattern closer to that seen in *Scd1* mRNA analysis (42, 43). A possible explanation for the source of these errors might come from cumulative pipetting errors during q-PCR sample loadings for these genes within the four replicas, this hypothesis is especially plausible as the affected genes were done in the same q-PCR plate. Therefore, unfortunately, due to high error in the samples and inconsistent expression pattern of the genes, no relevant tendency can be commented. Further experiments would be needed to elucidate the role of *Plcb3* in *de-novo* lipogenesis.

To evaluate the possible implications of Plcb3 in adipocyte proliferation, proliferation marker Ki67 is analysed. Following the results, *Ki67* mRNA and protein gene expression was also analysed to elucidate if *Plcb3* gene had an effect on adipocyte proliferation. Results for *Ki67* expression appear to be discordant between mRNA and protein results. Whilst mRNA expression appears to show how *Plcb3* group is upregulated for the gene, protein expression shows opposite tendencies. However, mRNA results appear to have less standard error in the most significant day of proliferation (Day 1) whilst protein results have overlapping standard error bars, therefore mRNA results will be more trustable, even though further validation of the results is needed. One possible reason behind the high standard error bars in protein analysis is that the antibody used did not allow for a clear detection of the protein bands, as the protein band intensity was closer to the background intensity.

To evaluate if earlier results translated onto visible morphological differences in adipocyte differentiation, immunofluorescence morphological analysis takes place. Morphological analysis results seem to further support what has been commented earlier in discussion. In first place the results seem to show a decrease in adipogenesis, observed as there seems to be a lower amount of lipid droplets marked by LipidTOX in red in the silenced group. These results would correlate with results seen for late adipogenesis genes mRNA and protein analysis where Plin1, Plin2 and Ap2 appeared to be downregulated in Plcb3 group. This means that, even though Plcb3 silencing appears to be slightly upregulating early adipogenesis genes (Pparγ2 and Cebpα), it has the opposite effect on later adipogenesis genes, resulting on the silencing having a result of lowering adipogenesis lipid droplet formation. In addition to this, immunofluorescence results appear to show how *Ki67* gene seems to be more expressed in the *Plcb3* group. This results further support *Ki67´*s mRNA expression profile over protein one and suggests possible implications of *Plcb3* regulating adipocytes proliferation. If the *Plcb3* silenced group had promoted proliferation, *Plcb3* could be a gene which suppresses proliferation. One possible explanation for this phenomenon is that Plcb3, supresses proliferation via AMPK signalling, were Plcb3 activates AMPK by calcium release of the ER reservoirs by IP3. There is bibliography supporting this showing how, in fact AMPK causes growth arrest at G1 phase by upregulation of p53-p21 axis and mTOR inhibition. AMPK activates p53 and p53 activates p21, which acts inhibiting CDK´s (cyclin dependent kinases), which are required for advancing on the cell cycle. At the same time AMPK inhibits mTOR via TSC protein activation (44). It is important to remember that the silencing done in this project was a knockdown, meaning that Plcb3´s expression is not fully impaired. As a result of this, the visible differences between groups might not be as evident, for instance, for Plin1 immunostaining, no visible difference is easily appreciated between conditions. However, it is important to note that for morphological analysis results, to get more evident results a fluorescence quantification would be needed to point out any possible actual differences between groups.

In conclusion, the presented results could point towards *Plcb3* having a dual role in downregulating initial steps of adipogenesis, whilst promoting later steps, based on earlier commented evidence (37, 40). The results show tendencies that point towards *Plcb3* having a role of promoting adipogenesis, as it influences adipogenesis related genes and lipid droplet development (*Plin1*, *Plin2* and *Ap2*) which is supported by mentioned bibliographical evidence (40). Furthermore, the gene appears to also have a negative effect on adipocyte proliferation possibly caused by its interaction with AMPK and its downstream signalling elements that result in growth arrest (44).

6. CONCLUSIONS

1. The bioinformatic analysis results obtained by processing the GEO GSE95533 dataset showed preliminarily how *Plcb3* gene in 3T3-L1 cells increased its expression on the later days of differentiation.
2. The *Plcb3* mRNA gene expression analysis showed a tendency in which expression would increase gradually until a maximum expression at day 5 of differentiation. Suggesting that *Plcb3* does express during adipogenesis.
3. The Plcb3 protein expression analysis showed a tendency similar to the mRNA results but the day of maximum expression was at day 3 of adipogenesis. Reinforcing how Plcb3 could be having its maximum peak of expression in early adipogenesis days.
4. The silencing of *Plcb3* appears to have a double effect on adipogenesis, on one side it appears to downregulate expression of early adipogenesis genes for initial days of adipogenesis and on the other side, it looks like the gene promotes the expression of late adipogenesis and lipid droplet formation genes. This could result in *Plcb3* being an adipogenesis promoting gene.
5. Silencing of *Plcb3* in mRNA expression and morphological analysis of *Ki67* show how the gene appears to be upregulated in silenced group. This shows how Plcb3 could have a role in inhibiting adipocyte proliferation.
6. Results regarding the effects of *Plcb3* silencing on *de-novo* adipogenesis are inconclusive and further research is needed to elucidate its role in this process.
7. Morphological analysis showed how adipocyte differentiation took place in both conditions, *Plcb3* condition having a lower number of lipid droplets than the control group. This further validates the hypothesis that Plcb3 has a role in promoting adipogenesis.

7. LIMITATIONS OF THE STUDY

One of the main limitations of the study was the number of experimental errors (mostly pipetting errors and errors during collection of RNA and protein samples) occurred during differentiation experiments, which were errors that were later transferred onto mRNA, protein or morphological analysis. In addition to this, the fact that the silencing was a knockdown and not a knockout possibly made less evident results in some cases, as the silencing of the gene is never 100%. Furthermore, cells used for the experiments were from a slightly high passage number, meaning that there could possibly be deviations in the normal expression of genes. Addressing and rectifying these problems could possibly have resulted in more statistically relevant results. This will be taken into account in future experiments.

BIBLIOGRAPHY

1. Si, Z., Wang, X., Sun, C., Kang, Y., Xu, J., Wang, X., & Hui, Y. (2019b). Adipose-derived stem cells: Sources, potency, and implications for regenerative therapies. Biomedicine & Pharmacotherapy, 114, 108765. https://doi.org/10.1016/j.biopha.2019.108765

2. Richard, A. J., White, U., Elks, C. M., & Stephens, J. M. (2020, 4 abril). Adipose Tissue: Physiology to Metabolic Dysfunction. Endotext - NCBI Bookshelf. https://www.ncbi.nlm.nih.gov/books/NBK555602/

3. Weger, M., Diotel, N., Dorsemans, A., Dickmeis, T., & Weger, B. (2017). Stem cells and the circadian clock. Developmental Biology, 431(2), 111-123. https://doi.org/10.1016/j.ydbio.2017.09.012

4. Talley, J. T., & Mohiuddin, S. S. (2023, 16 enero). Biochemistry, fatty acid oxidation. StatPearls - NCBI Bookshelf. https://www.ncbi.nlm.nih.gov/books/NBK556002/

5. Haas, B., Schlinkert, P., Mayer, P., & Eckstein, N. (2012). Targeting adipose tissue. Diabetology & Metabolic Syndrome, 4(1). https://doi.org/10.1186/1758-5996-4-43

6. Barbatelli, G., Murano, I., Madsen, L., Hao, Q., Jimenez, M., Kristiansen, K., Giacobino, J. P., De Matteis, R., & Cinti, S. (2010). The emergence of cold-induced brown adipocytes in mouse white fat depots is determined predominantly by white to brown adipocyte transdifferentiation. Endocrinology And Metabolism/American Journal Of Physiology: Endocrinology And Metabolism, 298(6), E1244-E1253. https://doi.org/10.1152/ajpendo.00600.2009

7. Ikeda, K., Maretich, P., & Kajimura, S. (2018b). The Common and Distinct Features of Brown and Beige Adipocytes. Trends In Endocrinology And Metabolism, 29(3), 191-200. https://doi.org/10.1016/j.tem.2018.01.001

8. Garin-Shkolnik, T., Rudich, A., Hotamisligil, G. S., & Rubinstein, M. (2014). FABP4 Attenuates PPARγ and Adipogenesis and Is Inversely Correlated With PPARγ in Adipose Tissues. Diabetes, 63(3), 900-911. https://doi.org/10.2337/db13-0436

9. Ghaben, A. L., & Scherer, P. E. (2019). Adipogenesis and metabolic health. Nature Reviews. Molecular Cell Biology, 20(4), 242-258. https://doi.org/10.1038/s41580-018-0093-z

10. Huang, S., & Czech, M. P. (2007). The GLUT4 glucose transporter. Cell Metabolism, 5(4), 237-252. https://doi.org/10.1016/j.cmet.2007.03.006

11. Sohn, J. H., Lee, Y. K., Han, J. S., Jeon, Y. G., Kim, J. I., Choe, S. S., Kim, S. J., Yoo, H. J., & Kim, J. B. (2018). Perilipin 1 (Plin1) deficiency promotes inflammatory responses in lean adipose tissue through lipid dysregulation. Journal Of Biological Chemistry/˜The Journal Of Biological Chemistry, 293(36), 13974-13988. https://doi.org/10.1074/jbc.ra118.003541

12. Bi, J., Xiang, Y., Chen, H., Liu, Z., Grönke, S., Kühnlein, R. P., & Huang, X. (2012). Opposite and redundant roles of the two Drosophila perilipins in lipid mobilization. Journal Of Cell Science, 125(15), 3568-3577. https://doi.org/10.1242/jcs.101329

13. Obesity: causes, consequences, treatments, and challenges. (2021). Journal Of Molecular Cell Biology/Journal Of Molecular Cell Biology, 13(7), 463-465. https://doi.org/10.1093/jmcb/mjab056

14. Chait, A., & Hartigh, L. J. D. (2020). Adipose Tissue Distribution, Inflammation and Its Metabolic Consequences, Including Diabetes and Cardiovascular Disease. Frontiers In Cardiovascular Medicine, 7. https://doi.org/10.3389/fcvm.2020.00022

15. Nedunchezhiyan, U., Varughese, I., Sun, A. R., Wu, X., Crawford, R., & Prasadam, I. (2022). Obesity, Inflammation, and Immune System in Osteoarthritis. Frontiers In Immunology, 13. https://doi.org/10.3389/fimmu.2022.907750

16. Safaei, M., Sundararajan, E. A., Driss, M., Boulila, W., & Shapi'i, A. (2021). A systematic literature review on obesity: Understanding the causes & consequences of obesity and reviewing various machine learning approaches used to predict obesity. Computers In Biology And Medicine, 136, 104754. https://doi.org/10.1016/j.compbiomed.2021.104754

17. Información de la Encuesta Europea de Salud en España del año 2020 y de la Encuesta Nacional de Salud del año 2017. (2020). Instituto Nacional de Estadística (INE). https://ine.es/ss/Satellite?c=INESeccion_C&cid=1259926457058&p=%5C&pagename=ProductosYServicios%2FPYSLayout¶m1=PYSDetalle¶m3=1259924822888

18. National Health and Nutrition Examination Survey, 2017-March 2020 Prepandemic File: Sample Design, Estimation, and Analytic Guidelines. (2022, 1 mayo). PubMed. https://pubmed.ncbi.nlm.nih.gov/35593699/

19. National Institute for Health and Care Excellence (NICE). (2023, 26 julio). Obesity: identification, assessment and management. NCBI Bookshelf. https://www.ncbi.nlm.nih.gov/books/NBK588750/

20. Acerca del índice de masa corporal para adultos. (2022, 29 agosto). Centers For Disease Control And Prevention. https://www.cdc.gov/healthyweight/spanish/assessing/bmi/adult_bmi/index.html#IMC

21. Callahan, E. A. (2023, 31 julio). The Science, Strengths, and Limitations of Body Mass Index. Translating Knowledge Of Foundational Drivers Of Obesity Into Practice - NCBI Bookshelf. https://www.ncbi.nlm.nih.gov/books/NBK594362/

22. Watanabe, K., Wilmanski, T., Diener, C., Earls, J. C., Zimmer, A., Lincoln, B., Hadlock, J. J., Lovejoy, J. C., Gibbons, S. M., Magis, A. T., Hood, L., Price, N. D., & Rappaport, N. (2023). Multiomic signatures of body mass index identify heterogeneous health phenotypes and responses to a lifestyle intervention. Nature Medicine, 29(4), 996-1008. https://doi.org/10.1038/s41591-023-02248-0

23. Huang, L. O., Rauch, A., Mazzaferro, E., Preuss, M., Carobbio, S., Bayrak, C. S., Chami, N., Wang, Z., Schick, U. M., Yang, N., Itan, Y., Vidal-Puig, A., Hoed, M. D., Mandrup, S., Kilpeläinen, T. O., & Loos, R. J. F. (2021). Genome-wide discovery of genetic loci that uncouple excess adiposity from its comorbidities. Nature Metabolism, 3(2), 228-243. https://doi.org/10.1038/s42255-021-00346-2

24. PLCB3 phospholipase C beta 3 [Homo sapiens (human)] - Gene - NCBI. (s. f.). https://www.ncbi.nlm.nih.gov/gene/5331

25. Bill, C. A., & Vines, C. M. (2019). Phospholipase C. En Advances in experimental medicine and biology (pp. 215-242). https://doi.org/10.1007/978-3-030-12457-1_9

26. Lyon, A. M., & Tesmer, J. J. G. (2013). Structural Insights into Phospholipase C-βFunction. Molecular Pharmacology, 84(4), 488-500. https://doi.org/10.1124/mol.113.087403

27. Dufau, J., Shen, J. X., Couchet, M., De Castro Barbosa, T., Mejhert, N., Massier, L., Griseti, E., Mouisel, E., Amri, E., Lauschke, V. M., Rydén, M., & Langin, D. (2021). In vitro and ex vivo models of adipocytes. American Journal Of Physiology. Cell Physiology, 320(5), C822-C841. https://doi.org/10.1152/ajpcell.00519.2020

28. Ruiz-Ojeda, F. J., Rupérez, A. I., Gomez-Llorente, C., Gil, A., & Aguilera, C. M. (2016). Cell Models and Their Application for Studying Adipogenic Differentiation in Relation to Obesity: A Review. International Journal Of Molecular Sciences, 17(7), 1040. https://doi.org/10.3390/ijms17071040

29. 3T3-L1 Cell Line: A Key to Understanding Obesity. (s. f.). Cytion. https://www.cytion.com/The-3T3-L1-Cell-Line-A-Key-to-Understanding-Obesity

30. Suleiman, J. B., Mohamed, M., & Bakar, A. B. A. (2020). A systematic review on different models of inducing obesity in animals: Advantages and limitations. Journal Of Advanced Veterinary And Animal Research, 7(1), 103. https://doi.org/10.5455/javar.2020.g399

31. Kfoury, S., Michl, P., & Roth, L. (2022). Modeling Obesity-Driven Pancreatic Carcinogenesis—A Review of Current In Vivo and In Vitro Models of Obesity and Pancreatic Carcinogenesis. Cells, 11(19), 3170. https://doi.org/10.3390/cells11193170

32. Company of Biologists. (2012, 1 septiembre). 'POKO mice' enable studies of obesity-associated kidney disease. PubMed Central (PMC). https://www.ncbi.nlm.nih.gov/pmc/articles/PMC3424443/

33. Siersbæk, R., Madsen, J. G. S., Javierre, B. M., Nielsen, R., Bagge, E. K., Cairns, J., Wingett, S. W., Traynor, S., Spivakov, M., Fraser, P., & Mandrup, S. (2017). Dynamic Rewiring of Promoter-Anchored Chromatin Loops during Adipocyte Differentiation. Molecular Cell, 66(3), 420-435.e5. https://doi.org/10.1016/j.molcel.2017.04.010

34. Dorsett, Y., & Tuschl, T. (2004). siRNAs: applications in functional genomics and potential as therapeutics. Nature Reviews. Drug Discover/Nature Reviews. Drug Discovery, 3(4), 318-329. https://doi.org/10.1038/nrd1345

35. What is Multiplicity of Infection (MOI)? (s. f.). Abmgood. https://info.abmgood.com/multiplicity-of-infection-moi

36. O'Carroll, S. J., Mitchell, M. D., Faenza, I., Cocco, L., & Gilmour, R. S. (2009). Nuclear PLC Beta 1 is required for 3T3-L1 adipocyte differentiation and regulates expression of the cyclin D3–cdk4 complex. Cellular Signalling, 21(6), 926-935. https://doi.org/10.1016/j.cellsig.2009.02.002

37. Zhou, Y., Wang, D., Li, F., Shi, J., & Song, J. (2006). Different roles of protein kinase C-βI and -δ in the regulation of adipocyte differentiation. International Journal Of Biochemistry & Cell Biology, 38(12), 2151-2163. https://doi.org/10.1016/j.biocel.2006.06.009

38. Lin, F., Ribar, T. J., & Means, A. R. (2011). The CA2+/Calmodulin-Dependent protein kinase kinase, CAMKK2, inhibits preadipocyte differentiation. Endocrinology, 152(10), 3668-3679. https://doi.org/10.1210/en.2011-1107

39. (2001). The Effects of AICAR on Adipocyte Differentiation of 3T3-L1 Cells. Biochemical And Biophysical Research Communications, 286(5), 852-856. https://doi.org/10.1006/bbrc.2001.5484

40. He, Y., He, Y., Liao, X., Niu, Y., Wang, G., Zhao, C., Wang, L., Tian, M., Li, Y., & Sun, C. (2011). The calcium-sensing receptor promotes adipocyte differentiation and adipogenesis through PPARγ pathway. Molecular And Cellular Biochemistry, 361(1-2), 321-328. https://doi.org/10.1007/s11010-011-1118-

41. Sanders, F. W. B., & Griffin, J. L. (2015). De novo lipogenesis in the liver in health and disease: more than just a shunting yard for glucose. Biological Reviews/Biological Reviews Of The Cambridge Philosophical Society, 91(2), 452-468. https://doi.org/10.1111/brv.12178

42. Juiz-Valiña, P., Varela-Rodríguez, B. M., Outeiriño-Blanco, E., García-Brao, M. J., Mena, E., Cordido, F., & Sangiao-Alvarellos, S. (2022). MiR-19 Family Impairs Adipogenesis by the Downregulation of the PPARγ Transcriptional Network. International Journal Of Molecular Sciences, 23(24), 15792. https://doi.org/10.3390/ijms232415792

43. Payne, V. A., Au, W., Lowe, C. E., Rahman, S. M., Friedman, J. E., O'Rahilly, S., & Rochford, J. J. (2009). C/EBP transcription factors regulate SREBP1c gene expression during adipogenesis. Biochemical Journal, 425(1), 215-224. https://doi.org/10.1042/bj20091112

44. Motoshima, H., Goldstein, B. J., Igata, M., & Araki, E. (2006). AMPK and cell proliferation – AMPK as a therapeutic target for atherosclerosis and cancer. Journal Of Physiology, 574(1), 63-71. https://doi.org/10.1113/jphysiol.2006.108324

ANEJO.1 RELACIÓN DEL TRABAJO CON LOS OBJETIVOS DE DESARROLLO SOSTENIBLE DE LA AGENDA 2030

UNIVERSITAT POLITÈCNICA DE VALÈNCIA

Escola Tècnica Superior d'Enginyeria Agronòmica i del Medi Natural

Anejo I. Relación del trabajo con los Objetivos de Desarrollo Sostenible de la agenda 2030.

A. Indicar el grado de relación del trabajo con los Objetivos de Desarrollo Sostenible (ODS).

	Alto	Medio	Bajo	No procede
ODS 1. Fin de la pobreza				X
ODS 2. Hambre cero				X
ODS 3. Salud y bienestar	x			
ODS 4. Educación de calidad				X
ODS 5. Igualdad de género				X
ODS 6. Agua limpia y saneamiento				X
ODS 7. Energía asequible y no contaminante				X
ODS 8. Trabajo decente y crecimiento económico				X
ODS 9. Industria, innovación e infraestructuras				X
ODS 10. Reducción de las desigualdades				X
ODS 11. Ciudades y comunidades sostenibles				X
ODS 12. Producción y consumo responsables				X
ODS 13. Acción por el clima				X
ODS 14. Vida submarina				X
ODS 15. Vida de ecosistemas terrestres				X
ODS 16. Paz, justicia e instituciones sólidas				X
ODS 17. Alianzas para lograr objetivos.				X

B. Describir brevemente la alineación del TFG con los ODS, marcados en la tabla anterior, con un grado alto.

Este proyecto va muy afín con el ODS N.º 3 de salud y bienestar. Esto se debe a que el objetivo del proyecto es caracterizar el posible papel que pueda tener un gen en el desarrollo de la grasa, con el fin ultimo de poder caracterizar de mejor manera a una de las condiciones más comunes hoy en día, la obesidad y que a su vez, esta relacionada con enfermedades como enfermedades cardiovasculares o la diabetes tipo 2.